

# Dispersive constraints on fermion masses

Hsiang-nan Li

*Institute of Physics, Academia Sinica, Taipei, Taiwan 115, Republic of China*

(Dated: May 3, 2023)

We demonstrate that fermion masses in the Standard Model (SM) can be constrained by the dispersion relations obeyed by hadronic and semileptonic decay widths of a fictitious heavy quark  $Q$  with an arbitrary mass. These relations, imposing stringent connections between high-mass and low-mass behaviors of decay widths, correlate a heavy quark mass and the chiral symmetry breaking scale. Given the known input from leading-order heavy quark expansion and a hadronic threshold for decay products, we solve for a physical heavy quark decay width. It is shown that the charm (bottom) quark mass  $m_c = 1.35$  GeV ( $m_b = 4.0$  GeV) can be determined by the dispersion relation for the  $Q \rightarrow dud\bar{}$  ( $Q \rightarrow c\bar{u}d$ ) decay with the threshold  $2m_\pi$  ( $m_\pi + m_D$ ), where  $m_\pi$  ( $m_D$ ) denotes the pion ( $D$  meson) mass. Requiring that the dispersion relation for the  $Q \rightarrow sud\bar{}$  ( $Q \rightarrow d\mu^+\nu_\mu$ ,  $Q \rightarrow u\tau^-\bar{\nu}_\tau$ ) decay with the threshold  $m_\pi + m_K$  ( $m_\pi + m_\mu$ ,  $m_\pi + m_\tau$ ) yields the same heavy quark mass,  $m_K$  being the kaon mass, we obtain the strange quark (muon,  $\tau$  lepton) mass  $m_s = 0.12$  GeV ( $m_\mu = 0.11$  GeV,  $m_\tau = 2.0$  GeV). Moreover, all the predicted decay widths corresponding to the above masses agree with the data. It is pointed out that our formalism is similar to QCD sum rules for probing resonance properties, and that the Pauli interference (weak annihilation) provides the higher-power effect necessary for establishing the solutions of the hadronic (semileptonic) decay widths. This work suggests that the parameters in the SM may not be free, but arranged properly to achieve internal dynamical consistency.

## I. INTRODUCTION

How to understand the flavor structures of the Standard Model (SM), such as the hierarchy of quark and lepton masses, and the dramatically different quark and lepton mixing patterns, has been a long-term pursuit in particle physics. Many proposals have been made in the literature, which usually rely on additional symmetries or interactions. For example, a flavor U(1) symmetry with a scalar field called flavon was introduced and then spontaneously broken in the Froggatt-Nielsen model [1]. The aforementioned flavor structures were generated in various models with modular flavor symmetry [2], which has attracted great attention [3–7]. The smooth confinement mechanism without chiral symmetry breaking [8–10] was implemented to explain the small Yukawa couplings of the first- and second-family fermions, which are composites of ultraviolet fields, while the third-family fermions are elementary to be consistent with the  $O(1)$  top Yukawa coupling [11]. Alternative scenarios, which do not resort to symmetries but to localizations of fermions in extra dimensions [12] or to the clockwork mechanism [13, 14], were also attempted. We will demonstrate, without any new ingredients beyond the SM, that at least the fermion masses around the GeV scale, including the strange quark, charm quark, bottom quark, muon and  $\tau$  lepton masses, may be understood through the internal consistency of SM dynamics.

We performed a dispersive analysis on the  $D$  meson mixing recently [15], starting with the transition matrix elements, which contain the flavor-changing four-quark operators in effective weak Hamiltonians, for a fictitious  $D$  meson of an arbitrary mass. Surprisingly, the solution to the dispersion relation obeyed by the transition matrix elements appears at the physical  $D$  meson mass  $m_D$ . The emergence of the scale  $m_D$  in the dispersive analysis inspires two speculations. First, an appropriate correlation function defined by the four-quark effective operators can be employed to establish the mass of a decaying heavy meson, similar to the determination of a light resonance mass that has been achieved extensively in QCD sum rules [16]. The heavy quark invariant mass squared in the dispersive analysis plays the role of the invariant momentum squared injected into a current operator in sum rules. The heavy quark expansion (HQE) for the evaluation of a heavy meson matrix element corresponds to the operator product expansion in sum rules. The distinction arises from the operators (four-quark operators in the former and currents in the latter) and the external states (heavy meson states in the former and the vacuum state in the latter), which sandwich the operators, for defining a correlation function. Second, the absorptive piece of the transition matrix elements receives contributions from various fictitious  $D$  meson decay channels. It is then likely to correlate a heavy quark mass and masses of its light decay products, which originate from the chiral symmetry breaking in QCD, through the dispersion relation. The above two speculations suggest the possibility of addressing at least partial flavor structure of the SM in the dispersive analysis on inclusive heavy quark decays.

We will study a hadronic matrix element of the four-quark effective operators, whose absorptive piece defines a decay width of a fictitious heavy quark  $Q$  with an arbitrary mass  $m_Q$ . The associated dispersion relation is derived, which imposes a stringent connection between the high-mass and low-mass behaviors of the decay width, and then solved directly, namely, treated as an inverse problem [17]. It has been proved rigorously [18] that a unique solution

exists for this type of integral equation, when boundary conditions are specified. The decay width at large  $m_Q$  approaches its HQE in powers of  $1/m_Q$ , which has been known to accommodate the observed  $B$  and  $B_s$  meson lifetimes well. It ought to vanish at a hadronic threshold, which originates from the chiral symmetry breaking for light quarks. This threshold depends on final states, taking, for instance,  $2m_\pi$  with the pion mass  $m_\pi$  for the channel involving only up and down quarks. Following the proposal in [19], we scale the dispersion relation by changing  $m_Q^2 = u\Lambda$  into a dimensionless variable  $u$ , which introduces the arbitrary scale  $\Lambda$ . A solution to the dispersion relation must not be affected by this artificial variable change. It turns out, given the boundary conditions at infinity and the threshold, that only when  $m_Q$  takes a specific value, can the stability with respect to the variation of  $\Lambda$  be realized.

It will be shown that the above specific  $m_Q$  solved from the dispersion relation does coincide with the mass of a physical heavy (charm or bottom) quark. We first perform the dispersive analysis of the hadronic decay  $Q \rightarrow dud\bar{d}$ , regarding the final-state up and down quarks as being massless, with the leading-order (LO) HQE input and the threshold  $2m_\pi$ . The pion mass  $m_\pi$  is a result of the chiral symmetry breaking in QCD as stated before. The charm quark mass  $m_c = 1.35$  GeV is then inferred, close to the value extracted from measured  $D$  meson lifetimes [20]. We then proceed to the investigation of the  $Q \rightarrow sud\bar{d}$  decay with the threshold  $m_\pi + m_K$ ,  $m_K$  being the kaon mass. It is encouraging to find that the strange quark mass  $m_s$  must take a value around  $m_s = 0.12$  GeV in order to produce the same charm quark mass from the  $Q \rightarrow dud\bar{d}$  analysis. The relation between  $m_s$  and  $m_K$  is governed by strong interaction as verified in lattice QCD [21] and sum rules [22]. The above observations indicate the internal consistency among the scales  $m_s$ ,  $m_\pi$ ,  $m_K$  and  $m_c$ , which characterize strong and weak dynamics in the SM. Moreover, the solved  $c \rightarrow s\bar{u}d$  decay width  $3.3 \times 10^{-13}$  GeV is reasonable, compared with the data of the Cabibbo-favored inclusive  $D^+$  meson decay modes [23]. The semileptonic decay  $Q \rightarrow d\mu^+\nu_\mu$  is examined in a similar manner by considering the threshold  $m_\pi + m_\mu$ ,  $m_\mu$  being the muon mass. It is noticed that the dispersive constraint on the muon mass is quite rigid, which must take the value  $m_\mu = 0.11$  GeV in order to generate the same charm quark mass.

We repeat the dispersive analysis on the width of the hadronic decay  $Q \rightarrow c\bar{u}d$  by inputting the charm quark mass  $m_c = 1.35$  GeV derived previously and the threshold  $m_\pi + m_D$ , which leads to the bottom quark mass  $m_b = 4.0$  GeV, consistent with the value extracted from measured  $B$  meson lifetimes [24]. The relation between  $m_c$  and  $m_D$  can be deduced in QCD, so no a priori information on the bottom quark is introduced. The predicted decay width at  $m_b = 4.0$  GeV also agrees with the  $b \rightarrow c\bar{u}d$  inclusive data in [23]. Demanding that the dispersion relation for the semileptonic decay  $Q \rightarrow u\tau^-\bar{\nu}_\tau$  with the threshold  $m_\pi + m_\tau$  gives the same bottom quark mass, we fix the  $\tau$  lepton mass  $m_\tau = 2.0$  GeV. To sum up, the above fermion masses can be determined, starting from massless up and down quarks, by the dispersion relations which correlate ultraviolet and infrared behaviors of meson weak decays. We point out that the solution for a decay width reduces to the HQE input, once the chiral symmetry is restored, and no constraint on fermion masses can be imposed. It is stressed that the Pauli interference (weak annihilation) provides the higher-power effect essential for establishing a solution of the hadronic (semileptonic) decay width. For this reason, the semileptonic decay into the  $e\nu_e$  final state does not serve the purpose of constraining the involved fermion masses efficiently because of the helicity suppression on weak annihilation.

The rest of the paper is organized as follows. We construct the dispersion relation obeyed by the absorptive piece of a heavy meson matrix element of the four-quark effective operators in Sec. II. The  $Q \rightarrow dud\bar{d}$  case with the LO HQE input for massless decay products is explored in detail to illustrate our formalism. The equation for specifying the physical heavy quark mass is presented as a consequence of the scale invariance in the arbitrary  $\Lambda$ , which generates the charm quark mass  $m_c$ . We study the  $Q \rightarrow sud\bar{d}$ ,  $Q \rightarrow c\bar{u}d$ ,  $Q \rightarrow d\mu^+\nu_\mu$  and  $Q \rightarrow u\tau^-\bar{\nu}_\tau$  decays into massive final states for fixing the masses  $m_s$ ,  $m_b$ ,  $m_\mu$  and  $m_\tau$ , respectively, in Sec. III. It is corroborated that the solved decay widths exhibit apparent stability under the variation of  $\Lambda$ , and match the data satisfactorily. Section IV contains the conclusion and outlook.

## II. DISPERSIVE CONSTRAINTS

The nonperturbative approach based on dispersion relations for physical observables was proposed in [17], and then applied to the constraint on the hadronic vacuum polarization contribution to the muon anomalous magnetic moment [25], to the reformulation of QCD sum rules for extracting properties of the series of  $\rho$  resonances [26], glueball masses [19] and the pion light-cone distribution amplitude [27], and to the explanation of the large observed  $D$  meson mixing parameters [15]. Here we will extend it to the analysis of heavy quark decay widths and demonstrate that the involved fermion masses can be constrained, as the hadronic thresholds are introduced into the relevant dispersion relations. We concentrate on the  $Q \rightarrow dud\bar{d}$  case with massless final-state quarks and the determination of the charm quark mass in this section.

### A. Dispersion Relation

Consider the analytical correlation function  $\Pi(m_Q)$  for a heavy meson  $H_Q$  of the mass  $m_{H_Q}$  formed by the fictitious heavy quark  $Q$ , which is defined by the matrix element

$$\Pi(m_Q) \equiv \frac{1}{2m_{H_Q}(m_Q)} \langle H_Q | \mathcal{T} | H_Q \rangle = M(m_Q) + i\Gamma(m_Q). \quad (1)$$

The transition operator  $\mathcal{T}$  is written as

$$\mathcal{T} = i \int d^4x T \left[ \mathcal{H}_{\text{eff}}^\dagger(x) \mathcal{H}_{\text{eff}}(0) \right], \quad (2)$$

where  $\mathcal{H}_{\text{eff}}$  denotes the  $\Delta Q = 1$  effective weak Hamiltonian. The functions  $M(m_Q)$  and  $\Gamma(m_Q)$  represent the dispersive and absorptive pieces, respectively. It has been observed that power corrections are crucial for establishing a resonance solution in QCD sum rules [26]. Hence, we stick to those heavy meson decays, which contain sizable higher-power corrections. It is known that the  $D^0$  meson lifetime receives a dimension-six contribution only from the  $W$ -exchange topology, which suffers chiral suppression under the vacuum insertion approximation [28]. It is possible to constrain the strange quark mass through the introduction of the  $m_s$ -dependent threshold into the dispersion relation, so we will not discuss  $D_s$  meson decays. We thus analyze  $D^+$  meson decays below, whose widths in the HQE have been available in the literature.

The inclusive hadronic (semileptonic) decay width of a charged heavy meson is written, in the HQE, as [24, 29, 30]

$$\Gamma_{h(s)}^{\text{HQE}}(m_Q) = \frac{G_F^2 |V_{\text{CKM}}|^2 m_Q^5}{192\pi^3} \left[ c_{h(s)}^{(3)} \left( 1 - \frac{\mu_\pi^2 - \mu_G^2}{2m_Q^2} \right) + 2c_{h(s)}^{(5)} \frac{\mu_G^2}{m_Q^2} + \Gamma_{h(s)}^{(6)+(7)}(m_Q) \right], \quad (3)$$

where  $G_F$  is the Fermi constant and  $V_{\text{CKM}}$  represents the Cabibbo-Kobayashi-Maskawa (CKM) factor. The heavy-quark-effective-theory (HQET) parameters  $\mu_\pi^2$  and  $\mu_G^2$  are defined by the matrix elements  $\langle H_Q | \bar{Q}Q | H_Q \rangle$  and  $\langle H_Q | \bar{Q} \sigma_{\mu\nu} G^{\mu\nu} Q | H_Q \rangle$ , respectively, with the gluon field strength  $G^{\mu\nu}$ . The significance of the Darwin term is still uncertain, which depends on how it is extracted [31]. Here we do not take it into account according to [32]: a small Darwin contribution, consistent with zero basically, yields a better fit to the measured lifetime ratio  $\tau(B_s)/\tau(B_d)$ . The coefficient functions of the penguin operators vanish at LO in the strong coupling  $\alpha_s$ , the precision we will work on. It has been postulated that the HQE can be truncated to a good approximation after the dimension-seven terms [28], as done in Eq. (3).

For our purpose, it suffices to adopt the LO expressions for the hard coefficients [33]

$$\begin{aligned} c_h^{(3)} &= A_0(\mu) I_0(x_q), & c_h^{(5)} &= -A_0(\mu) I_1(x_q) - A_2(\mu) I_2(x_q), \\ c_s^{(3)} &= I_0(x_\ell), & c_s^{(5)} &= -I_1(x_\ell), \end{aligned} \quad (4)$$

with the ratios  $x_q = m_q^2/m_Q^2$  and  $x_\ell = m_\ell^2/m_Q^2$ ,  $m_q$  ( $m_\ell$ ) being the mass of a final-state quark  $q = s$  or  $c$  (charged lepton  $\ell = \mu$  or  $\tau$ ), which will be touched on in the next section. The functions  $A_i$  depend on the Wilson coefficients  $C_{1,2}$ ,

$$A_0 = N_c C_1^2 + N_c C_2^2 + 2C_1 C_2, \quad A_2 = 8C_1 C_2. \quad (5)$$

The functions  $I_i$  are given by [34, 35]

$$\begin{aligned} I_0(x) &= 1 - 8x + 8x^3 - x^4 - 12x^2 \ln x, \\ I_1(x) &= (1-x)^4, \quad I_2(x) = (1-x)^3. \end{aligned} \quad (6)$$

The next-to-leading-order (NLO) corrections to  $c^{(3)}$  can be found in Refs. [34, 36–40].

The term  $\Gamma_{h(s)}^{(6)+(7)}(m_Q)$  combines the dimension-six and -seven hard spectator contributions, including that from the Pauli interference (weak annihilation). The coefficient functions of the dimension-six operators for the hadronic decays were evaluated to LO in Refs. [41–43], and to NLO in Refs. [44, 45]. The dimension-seven contributions were computed only partially to LO in [20, 24, 28, 46]. The LO results are summarized as

$$\Gamma_h^{(6)+(7)}(m_Q) = 16\pi^2 \frac{f_{H_Q}^2 m_{H_Q}}{m_Q^3} (C_1^2 + C_2^2 + 2N_c C_1 C_2) (1-x_q)^2 \left[ 1 - \left( \frac{1+x_q}{1-x_q} + \frac{1}{2} \right) \frac{2\bar{\Lambda}}{m_Q} \right], \quad (7)$$

$$\Gamma_s^{(6)+(7)}(m_Q) = 16\pi^2 \frac{f_{H_Q}^2 m_{H_Q}}{m_Q^3} x_\ell (1-x_\ell) \left[ \frac{3}{2} (1-x_\ell) - 3x_\ell (1-2x_\ell) \frac{2\bar{\Lambda}}{m_Q} \right], \quad (8)$$

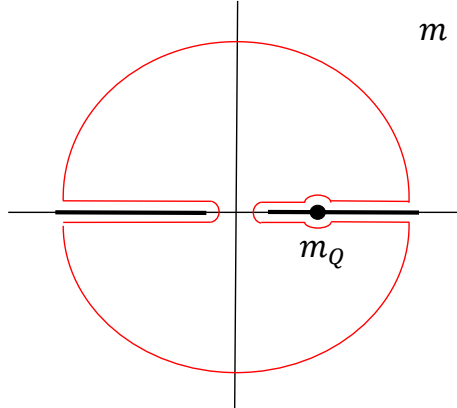


FIG. 1: Contour for Eq. (9), where the thick lines represent the branch cuts.

with the heavy meson decay constant  $f_{H_Q}$  and the binding energy  $\bar{\Lambda} = m_{H_Q} - m_Q$ . The vacuum insertion approximations for the involved hadronic matrix elements have been applied to simplify the expressions, and the weak annihilation contribution to the hadronic decay width is negligible compared with the Pauli interference one. Notice the two-body phase-space enhancement factor  $16\pi^2$  relative to the three-body phase space. This clarifies why the spectator effects, despite being power suppressed, are important.

Since the HQE result contains terms in various powers of  $1/m_Q$ , instead of in  $1/m_Q^2$ , the construction of a dispersion relation begins with the contour integration in the complex  $m_Q$  plane [47], instead of the  $m_Q^2$  plane [15], which possesses different branching cuts. We have the identity

$$\frac{1}{2\pi i} \oint dm \frac{\Pi(m)}{m_Q - m} = 0, \quad (9)$$

in which the contour consists of two pieces of horizontal lines above and below the branch cut along the positive real axis, two pieces of horizontal lines above and below the branch cut along the negative real axis, a small circle around the pole  $m = m_Q$  located on the positive real axis and a circle  $C_R$  of the large radius  $R$  as depicted in Fig. 1. The radius  $R$  should not exceed the  $W$  boson mass  $m_W$  in order to validate the use of the effective weak Hamiltonians in Eq. (2). The integral in Eq. (9) vanishes, for the contour encloses only unphysical regions without poles.

The contribution along the small clockwise circle yields  $M(m_Q)$ , and those from the four pieces of horizontal lines lead to the dispersive integrals of  $\Gamma(m)$ . Equation (9) becomes

$$M(m_Q) = \frac{1}{\pi} \int_{m_F}^R dm \frac{\Gamma(m)}{m_Q - m} - \frac{1}{\pi} \int_{-R}^{-m_F} dm \frac{\Gamma(m)}{m_Q - m} + \frac{1}{2\pi i} \int_{C_R} dm \frac{\Pi^{\text{HQE}}(m)}{m_Q - m}, \quad (10)$$

where the hadronic threshold  $m_F$  sums the masses in the lightest final state. The unknown function  $\Gamma(m)$  acquires nonperturbative contributions from the small  $m$  region, where the chiral symmetry is broken. It is the reason why the threshold  $m_F$ , which is dynamically generated and of order of the QCD scale  $\Lambda_{\text{QCD}}$ , appears in Eq. (10). The integrand  $\Pi(m)$ , taking values along the large counterclockwise circle  $C_R$ , can be reliably replaced by the perturbative one  $\Pi^{\text{HQE}}(m)$ ; as stated before, the HQE accounts for the measured  $B$  meson lifetimes well.

The dispersive part  $M^{\text{HQE}}(m_Q)$  and the absorptive part  $\Gamma^{\text{HQE}}(m_Q)$  from the HQE respect the dispersion relation,

$$M^{\text{HQE}}(m_Q) = \frac{1}{\pi} \int_0^R dm \frac{\Gamma^{\text{HQE}}(m)}{m_Q - m} - \frac{1}{\pi} \int_{-R}^0 dm \frac{\Gamma^{\text{HQE}}(m)}{m_Q - m} + \frac{1}{2\pi i} \int_{C_R} dm \frac{\Pi^{\text{HQE}}(m)}{m_Q - m}, \quad (11)$$

where the thresholds for the first two integrals on the right-hand side have been set to zero for the massless up and down quarks with  $m_q = 0$ . There is no pole at  $m_Q = 0$  up to the power shown in Eq. (3). Though  $\Gamma^{\text{HQE}}(m)$  does not describe the low-mass behavior of a physical decay width correctly, Eq. (11) holds simply owing to the analyticity of the perturbative quark-level calculation. We equate  $M(m_Q)$  and  $M^{\text{HQE}}(m_Q)$ , i.e., Eqs. (10) and (11) at large enough

$m_Q \gg m_F$ , arriving at

$$\int_{m_F}^R \frac{\Gamma(m)}{m_Q - m} dm - \int_{-R}^{-m_F} \frac{\Gamma(m)}{m_Q - m} dm = \int_0^R \frac{\Gamma^{\text{HQE}}(m)}{m_Q - m} dm - \int_{-R}^0 \frac{\Gamma^{\text{HQE}}(m)}{m_Q - m} dm, \quad (12)$$

where the contributions from the large circle  $C_R$  on the two sides have been canceled.

### B. Solution of Decay Width

We decompose the HQE hadronic width  $\Gamma_h^{\text{HQE}}(m)$  into the pieces, which are even and odd in powers of  $m$ ,  $\Gamma_h^{\text{HQE}}(m) = \Gamma_e^{\text{HQE}}(m) + \Gamma_o^{\text{HQE}}(m)$ , and the unknown function into  $\Gamma_h(m) = \Gamma_e(m) + \Gamma_o(m)$  accordingly. For the even piece, the variable change  $m \rightarrow -m$  applied to the second integrals on both sides of Eq. (12) results in

$$\int_{m_F^2}^{R^2} \frac{\Gamma_e(m)}{m_Q^2 - m^2} dm^2 = \int_0^{R^2} \frac{\Gamma_e^{\text{HQE}}(m)}{m_Q^2 - m^2} dm^2. \quad (13)$$

Moving the integrand on the right-hand side to the left-hand side, and regarding it as a subtraction term, we get

$$\int_0^\infty \frac{\Delta\Gamma_e(m)}{m_Q^2 - m^2} dm^2 = 0. \quad (14)$$

The subtracted unknown function  $\Delta\Gamma_e(m) \equiv \Gamma_e(m) - \Gamma_e^{\text{HQE}}(m)$  is fixed to  $-\Gamma_e^{\text{HQE}}(m)$  in the interval  $(0, m_F)$  of  $m$ , and approaches zero at large  $m$ , because of  $\Gamma_e(m) \rightarrow \Gamma_e^{\text{HQE}}(m)$  in this limit. Though  $R$  should not exceed  $m_W$ , we extend it to infinity owing to the diminishing of  $\Delta\Gamma_e(m)$  at large  $m$ .

For the odd piece in  $m$ , the variable change  $m \rightarrow -m$  applied to the second integrals on both sides of Eq. (12) gives

$$m_Q \int_{m_F^2}^{R^2} \frac{\Gamma_o(m)}{m(m_Q^2 - m^2)} dm^2 = m_Q \int_0^{R^2} \frac{\Gamma_o^{\text{HQE}}(m)}{m(m_Q^2 - m^2)} dm^2. \quad (15)$$

Moving the integrand on the right-hand side to the left-hand side leads to

$$\int_0^\infty \frac{\Delta\Gamma_o(m)}{m(m_Q^2 - m^2)} dm^2 = 0. \quad (16)$$

The subtracted unknown function  $\Delta\Gamma_o(m) \equiv \Gamma_o(m) - \Gamma_o^{\text{HQE}}(m)$  is fixed to  $-\Gamma_o^{\text{HQE}}(m)$  in the interval  $(0, m_F)$ , and approaches zero at large  $m$ . The implication of Eqs. (14) and (16) will be probed below. Since they hold for an arbitrary large scale  $m_Q$ , they impose a stringent correlation between the nonperturbative behavior of  $\Gamma_h(m)$  at low mass and the perturbative behavior of  $\Gamma_h(m) \approx \Gamma_h^{\text{HQE}}(m)$  at high mass, thus among the relevant mass scales. It is obvious that the trivial solutions  $\Delta\Gamma_{e,o}(m) = 0$ , i.e.,  $\Gamma_h(m) = \Gamma_h^{\text{HQE}}(m)$  exist as  $m_F \rightarrow 0$ . In other words, there will be no constraint on fermion masses in the absence of the chiral symmetry breaking. We emphasize that Eqs. (14) and (16) hold for each decay channel of  $H_Q$ , because the associated CKM factor can vary independently from a mathematical point of view.

We change  $m_Q^2$  and  $m^2$  in Eq. (14) into the dimensionless variables  $u$  and  $v$  via  $m_Q^2 = u\Lambda$  and  $m^2 = v\Lambda$ , respectively, obtaining

$$\int_0^\infty dv \frac{\Delta\Gamma_e(v)}{u - v} = 0. \quad (17)$$

The purpose of introducing the arbitrary scale  $\Lambda$  will become clear shortly. Viewing the fact that  $\Delta\Gamma_e(v)$  decreases at large  $v$ , and the major contribution to Eq. (17) arises from the region with finite  $v$ , we are allowed to expand Eq. (17) into a power series in  $1/u$  for sufficiently large  $u$  by inserting

$$\frac{1}{u - v} = \sum_{i=1}^{\infty} \frac{v^{i-1}}{u^i}. \quad (18)$$

Equation (17) then demands a vanishing coefficient for every power of  $1/u$ .

We start with the case of  $N$  vanishing coefficients,

$$\int_0^\infty dv v^{i-1} \Delta\Gamma_e(v) = 0, \quad i = 1, 2, 3 \dots, N, \quad (19)$$

where  $N$  is a large integer, such that Eq. (17) is valid up to negligible corrections down by a power  $1/u^{N+1}$ . It hints that  $\Delta\Gamma_e(v)$  can be expanded in terms of the generalized Laguerre polynomials  $L_j^{(\alpha)}(v)$  with the support  $[0, \infty)$ , which respect the orthogonality condition

$$\int_0^\infty v^\alpha e^{-v} L_i^{(\alpha)}(v) L_j^{(\alpha)}(v) dv = \frac{\Gamma(i + \alpha + 1)}{i!} \delta_{ij}. \quad (20)$$

The first  $N$  polynomials  $L_0^{(\alpha)}(v)$ ,  $L_1^{(\alpha)}(v)$ ,  $L_2^{(\alpha)}(v)$ ,  $\dots$ ,  $L_{N-1}^{(\alpha)}(v)$  are composed of the terms  $1$ ,  $v$ ,  $v^2$ ,  $\dots$ ,  $v^{N-1}$  appearing in Eq. (19). Therefore, the expansion of  $\Delta\Gamma_e(v)$  contains the polynomials with degrees  $j$  not lower than  $N$ ,

$$\Delta\Gamma_e(v) = \sum_{j=N}^{N'} a_j v^\alpha e^{-v} L_j^{(\alpha)}(v), \quad N' > N, \quad (21)$$

with a set of unknown coefficients  $a_j$ . The highest degree  $N'$  can be fixed by the initial condition  $\Delta\Gamma_e(v) = -\Gamma_e^{\text{HQE}}(v)$  in the interval  $(0, m_F^2/\Lambda)$  of  $v$ . Since  $-\Gamma_e^{\text{HQE}}(v)$  is a smooth function,  $N'$  needs not be infinite.

A generalized Laguerre polynomial takes the approximate form for a large  $j$  [48]

$$L_j^{(\alpha)}(v) \approx j^{\alpha/2} v^{-\alpha/2} e^{v/2} J_\alpha(2\sqrt{jkv}), \quad (22)$$

up to corrections of  $1/\sqrt{j}$ ,  $J_\alpha$  being a Bessel function of the first kind. Equation (21) becomes

$$\Delta\Gamma_e(m) \approx \sum_{j=N}^{N'} a_j \sqrt{\frac{jm^2}{\Lambda}} e^{-m^2/(2\Lambda)} J_\alpha\left(2\sqrt{\frac{jm^2}{\Lambda}}\right), \quad (23)$$

where the variable  $v$  has been written as  $m^2/\Lambda$  explicitly. Defining the scaling variable  $\omega \equiv \sqrt{N/\Lambda}$ , we have the approximation  $N'/\Lambda = \omega^2 + (N' - N)/N \approx \omega^2$  for a finite  $N' - N$ . Equation (23) then reduces to

$$\Delta\Gamma_e(m) \approx y_e (\omega m)^\alpha J_\alpha(2\omega m), \quad (24)$$

where the common Bessel functions  $J_\alpha(2\sqrt{jm^2/\Lambda}) \approx J_\alpha(2\omega m)$  for  $j = N, N+1, \dots, N'$  have been factored out, and the sum of the unknown coefficients  $\sum_{j=N}^{N'} a_j$  has been denoted by  $y_e$ . The exponential suppression factor  $e^{-s/(2\Lambda)} = e^{-\omega^2 m^2/(2N)}$  has been replaced by unity for a large  $N$  in the region with finite  $m$  and  $\omega$ , which we are interested in (see the next subsection). The correction to this replacement is of power  $1/N$ , smaller than that to Eq. (22).

We replicate the above procedure for Eq. (16), deriving

$$\frac{\Delta\Gamma_o(m)}{m} \approx y_o (\omega m)^\alpha J_\alpha(2\omega m), \quad (25)$$

with the same index  $\alpha$  as seen in the next subsection. A solution of the  $Q \rightarrow d\bar{u}\bar{d}$  decay width is thus expressed, in terms of a single Bessel function, as

$$\Delta\Gamma_h(m_Q) = \Delta\Gamma_e(m_Q) + \Delta\Gamma_o(m_Q) \approx y_e \left(1 + \frac{y_o}{y_e} m_Q\right) (\omega m_Q)^\alpha J_\alpha(2\omega m_Q). \quad (26)$$

We stress that a solution to the dispersion relation should be insensitive to the variation of the arbitrary scale  $\Lambda$ , which is introduced via the artificial variable changes. The variation of  $\Lambda$  is translated into that of  $\omega$ . To explain how to realize this insensitivity, we make a Taylor expansion of  $\Delta\Gamma_h(m_Q)$ ,

$$\Delta\Gamma_h(m_Q) = \Delta\Gamma_h(m_Q)|_{\omega=\bar{\omega}} + \frac{d\Delta\Gamma_h(m_Q)}{d\omega} \Big|_{\omega=\bar{\omega}} (\omega - \bar{\omega}) + \frac{1}{2} \frac{d^2\Delta\Gamma_h(m_Q)}{d\omega^2} \Big|_{\omega=\bar{\omega}} (\omega - \bar{\omega})^2 + \dots, \quad (27)$$

where the constant parameter  $\bar{\omega}$ , together with  $\alpha$ ,  $y_e$  and  $y_o$ , are determined via the fit of the first term  $\Delta\Gamma_h(m_Q)|_{\omega=\bar{\omega}}$  to  $-\Gamma_h^{\text{HQE}}(m_Q)$  in the interval  $(0, m_F)$  of  $m_Q$ .

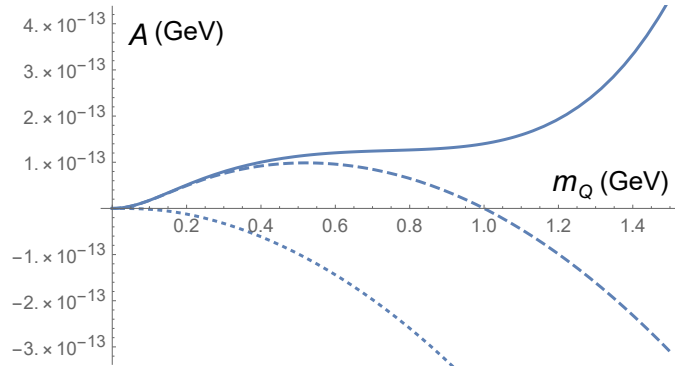


FIG. 2: The HQE hadronic decay width without the CKM factor,  $A(m_Q) \equiv \Gamma_h^{\text{HQE}}(m_Q)/|V_{\text{CKM}}|^2$ , from the dimension-six contribution (dotted line) only, from the sum of the dimension-six and -seven contributions (dashed line), and from the total contributions (solid line).

The insensitivity to the scaling variable  $\omega$  requires the vanishing of the first derivative in Eq. (27),

$$\left. \frac{d\Delta\Gamma_h(m_Q)}{d\omega} \right|_{\omega=\bar{\omega}} = 0, \quad (28)$$

from which roots of  $m_Q$  are solved. Furthermore, the second derivative  $d^2\Delta\Gamma_h(m_Q)/d\omega^2|_{\omega=\bar{\omega}}$  should be minimal to maximize the stability window around  $\bar{\omega}$ , in which  $\Delta\Gamma_h(m_Q)$  is almost independent of the variation of  $\omega$ . Because the HQE result is independent of  $\omega$ , the stability of  $\Delta\Gamma_h(m_Q)$  is equivalent to the stability of the decay width  $\Gamma_h(m_Q)$ . It will be shown that only when  $m_Q$  takes a specific value can the above requirements be met. Equation (26) with this specific  $m_Q$  establishes a solution to the dispersion relation in Eq. (12) with the initial condition in the interval  $(0, m_F)$  of  $m_Q$ . This specific  $m_Q$  will be identified as the physical heavy quark mass, at which the corresponding  $\Gamma_h = \Delta\Gamma_h + \Gamma_e^{\text{HQE}}$  represents our prediction for the considered decay width. Once a solution for the decay width is found, the degree  $N$  for the polynomial expansion in Eq. (21) can be pushed, together with the scale  $\Lambda$ , to arbitrarily large values by keeping the scaling variable  $\omega = \sqrt{N/\Lambda}$  within the stability window. Then all the arguments based on the large  $N$  scenario, including the neglect of the exponential factor  $e^{-m_Q^2/\Lambda}$  in Eq. (23), are justified. It has been observed in the investigation of neutral meson mixing [15] that the optimal choice of  $N$  for the polynomial expansion indeed increases with  $\Lambda$  in the stability window.

### C. Charm Mass from the $Q \rightarrow du\bar{d}$ Decay Width

We deduce the charm quark mass from the dispersion relation for the hadronic decay  $Q \rightarrow du\bar{d}$ , taking the Fermi constant  $G_F = 1.1663788 \times 10^{-5} \text{ GeV}^{-2}$ . Strictly speaking, the decay constant  $f_{H_Q}$  depends on the fictitious meson mass  $m_{H_Q}$ . However, the decay constants of the physical pseudoscalar mesons do not vary much in the low mass region, ranging from  $m_\pi \approx 0.14 \text{ GeV}$  to  $m_{B_s} \approx 5.4 \text{ GeV}$ . Hence, we treat  $f_{H_Q}$  as a constant, and set it to a typical value  $f_{H_Q} = 0.2 \text{ GeV}$ . The expansion for the heavy meson mass  $m_{H_Q} = m_Q + \bar{\Lambda}$  in Eq. (7) is implemented. The contribution down by the power  $\bar{\Lambda}/m_Q$  from the dimension-six term is then grouped into the dimension-seven one. The HQET parameters  $\bar{\Lambda}$ ,  $\mu_\pi^2$  and  $\mu_G^2$  vary with  $m_Q$  in principle. We also treat them as constants, and verify that outcomes have a weak dependence on them. We take  $\bar{\Lambda} = 0.5 \text{ GeV}$ ,  $\mu_\pi^2 = 0.43 \text{ GeV}^2$  and  $\mu_G^2 = 0.38 \text{ GeV}^2$ , i.e., the central values of the ranges inferred from the evaluations of  $B$  and  $D$  meson lifetimes [20, 31, 32, 49, 50]

$$\bar{\Lambda} = 0.5 \pm 0.1 \text{ GeV}, \quad \mu_\pi^2 = 0.43 \pm 0.24 \text{ GeV}^2, \quad \mu_G^2 = 0.38 \pm 0.07 \text{ GeV}^2. \quad (29)$$

The renormalization group evolution of the Wilson coefficients  $C_1(\mu)$  and  $C_2(\mu)$  with  $\mu = m_Q$  is taken into account to the leading logarithmic accuracy [51]. The fictitious quark mass can run to a very low scale in the  $Q \rightarrow du\bar{d}$  case. To stabilize the running coupling constant which the Wilson coefficients depend on, we introduce an effective gluon mass  $m_g$  into its argument:

$$\alpha_s(\mu) = \frac{4\pi}{\beta_0 \ln[(\mu^2 + m_g^2)/\Lambda_{\text{QCD}}^2]}, \quad (30)$$

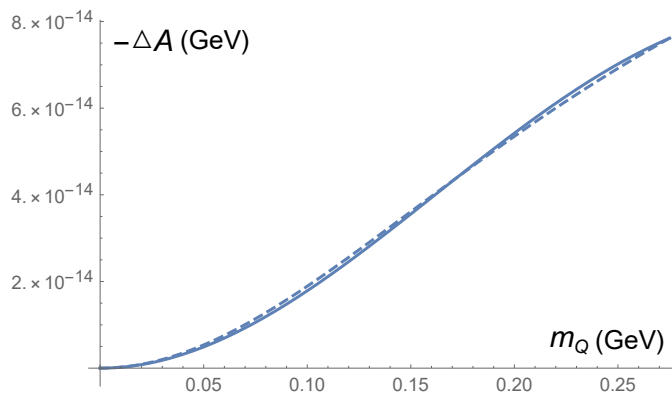


FIG. 3: Comparison of  $\Delta\Gamma_h(m_Q)$  in Eq. (33) from the fit (solid line) with  $-\Gamma_h^{\text{HQE}}(m_Q)$  (dashed line) in terms of the width without the CKM factor,  $\Delta A(m_Q) \equiv \Delta\Gamma_h^{\text{HQE}}(m_Q)/|V_{\text{CKM}}|^2$ .

with the coefficient  $\beta_0 = 11 - 2n_f/3$ . We adopt the one-loop running with the QCD scale  $\Lambda_{\text{QCD}} = 0.324$  GeV [52] for the number of active quark flavors  $n_f = 3$ . The effective gluon mass has been estimated to be about  $m_g \approx 0.4$  GeV [53, 54]. We choose  $m_g = 0.41$  GeV, and the reason for this choice will be provided later.

The relative importance of various contributions to the HQE hadronic width in Eq. (3) without the CKM factor,  $A(m_Q) \equiv \Gamma_h^{\text{HQE}}(m_Q)/|V_{\text{CKM}}|^2$ , is displayed in Fig. 2. The dimension-six Pauli interference effect gives a negative contribution due to the combination of the Wilson coefficients  $C_1^2 + C_2^2 + 2N_c C_1 C_2 < 0$  at a small scale [24]. The addition of the dimension-seven contribution turns the width positive up to the mass  $m_Q \approx 1$  GeV. The decay width becomes positive definite, after all the contributions are included. The sum of the dimension-six and -seven contributions dominates the low mass region with  $m_Q < 0.4$  GeV. Therefore, we have the approximate  $Q \rightarrow du\bar{d}$  HQE width at small  $m_Q$ ,

$$\Gamma_h^{\text{HQE}}(m_Q) \approx \Gamma_h^{(6)+(7)}(m_Q) \propto m_Q^3 - 2\bar{\Lambda}m_Q^2. \quad (31)$$

Utilizing  $J_\alpha(x) \sim (x/2)^\alpha/\Gamma(\alpha+1)$  as  $x \rightarrow 0$ , and comparing Eqs. (26) and (31) at low  $m_Q$ , we identify the index  $\alpha = 1$  from the limiting behavior  $\Gamma_h^{\text{HQE}} \propto m_Q^2$ , and the ratio

$$\frac{y_o}{y_e} = -\frac{1}{2\bar{\Lambda}} = -1 \text{ GeV}^{-1}. \quad (32)$$

The coefficient  $y_e$  is fixed by the boundary condition  $\Delta\Gamma_h(m_F) = -\Gamma_h^{\text{HQE}}(m_F)$  at  $m_Q = m_F$ , which leads the solution in Eq. (26) to

$$\Delta\Gamma_h(m_Q) = -\Gamma_h^{\text{HQE}}(m_F) \left(1 - \frac{m_Q}{2\bar{\Lambda}}\right) \left(1 - \frac{m_F}{2\bar{\Lambda}}\right)^{-1} \frac{m_Q J_1(2\omega m_Q)}{m_F J_1(2\omega m_F)}. \quad (33)$$

The best fit of Eq (33) to  $-\Gamma_h^{\text{HQE}}(m_Q)$  in the interval  $(0, m_F)$ ,  $m_F = m_{\pi^+} + m_{\pi^0}$  with the pion masses  $m_{\pi^+} = 0.140$  GeV and  $m_{\pi^0} = 0.135$  GeV, sets  $\omega = \bar{\omega} = 3.166 \text{ GeV}^{-1}$ . We contrast the fit result with  $-\Gamma_h^{\text{HQE}}(m_Q)$  in terms of the width without the CKM factor,  $\Delta A(m_Q) \equiv \Delta\Gamma_h^{\text{HQE}}(m_Q)/|V_{\text{CKM}}|^2$ , in Fig. 3. The excellent agreement confirms that the simple solution in Eq. (26) works well, and that other methods for determining  $\bar{\omega}$ , such as equating Eq. (33) and  $-\Gamma_h^{\text{HQE}}(m_Q)$  at  $m_Q = m_F/2$ , yield similar  $\bar{\omega}$ ; this equality produces  $\bar{\omega} = 3.280 \text{ GeV}^{-1}$ , close to the one from the best fit.

As elaborated before, the charm quark mass takes the physical value  $m_c$  that vanishes the first derivative in Eq. (28), namely,

$$D_1(m_Q) \equiv \frac{d}{d\omega} \frac{J_1(2\omega m_Q)}{J_1(2\omega m_F)} \Big|_{\omega=\bar{\omega}} = 0, \quad (34)$$

where the factors independent of  $\omega$  in Eq. (33) have been removed. At the same time, the second derivative

$$D_2(m_Q) \equiv \frac{d^2}{d\omega^2} \frac{J_1(2\omega m_Q)}{J_1(2\omega m_F)} \Big|_{\omega=\bar{\omega}}, \quad (35)$$



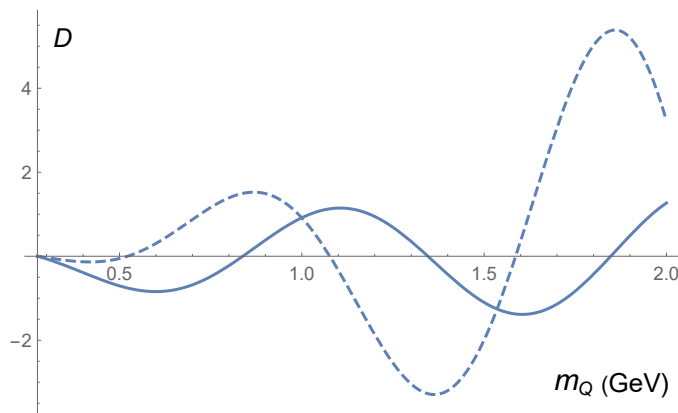


FIG. 4: Dependencies of the first derivative  $D_1(m_Q)$  (in units of GeV, solid line) in Eq. (34) and the second derivative  $D_2(m_Q)$  (in units of  $\text{GeV}^2$ , dashed line) in Eq. (35) on  $m_Q$ .

should be minimal as  $m_Q = m_c$ . Figure 4 presents the dependence of the first derivative in Eq. (34) on  $m_Q$ , which reveals several roots of  $m_Q$  in the small  $m_Q$  region. The first root located at  $m_Q = m_F = 0.275$  GeV, attributed to the boundary condition of  $\Delta\Gamma_h(m_Q)$  at this  $m_Q$ , is trivial and bears no physical significance. The dashed curve for Eq. (35) in Fig. 4 manifests a larger second derivative for, i.e., worse stability associated with a higher root, so a smaller root is preferred for  $m_c$ . It is known that a charm quark can decay into two strange quarks with the hadronic threshold  $2m_K \approx 1$  GeV. The second root at  $m_Q = 0.84$  GeV seems too low to be physical. We thus select the third root at  $m_Q = 1.35$  GeV as the physical solution of the charm quark mass, which implies the  $D^+$  meson mass  $m_{D^+} = m_c + \bar{\Lambda} = 1.85$  GeV in accordance with the measured value 1.870 GeV [55]. Another support for this choice is that the corresponding decay width agrees with the data as shown later. Our solution of  $m_c = 1.35$  GeV is consistent with the  $\overline{\text{MS}}$ , kinematic and pole masses of a charm quark, which are all equivalent at LO, and range between 1.28 GeV to 1.49 GeV at one loop [20].

We examine the sensitivity of the extracted charm quark mass to the variation of the involved inputs. The result has a weak dependence on the HQET parameters  $\bar{\Lambda}$ ,  $\mu_\pi$  and  $\mu_G$ . Taking the binding energy  $\bar{\Lambda}$  as the representative example, we find that the lower (upper) bound of the binding energy  $\bar{\Lambda} = 0.4$  GeV (0.6 GeV) generates the solution  $m_c = 1.37$  GeV (1.34 GeV). That is, 20% change of  $\bar{\Lambda}$  makes an impact of less than 2% on  $m_c$ . The variation of the decay constant  $f_{H_Q}$  has a similar effect: a smaller (larger) value  $f_{H_Q} = 0.16$  GeV (0.24 GeV) leads to  $m_c = 1.37$  GeV (1.33 GeV). Once the chiral symmetry is broken, up and down quarks should become massive too. We thus check the dependence on light quark masses by including the down quark mass  $m_d = 5$  MeV into the calculation, and assure that it has little influence on the outcome; the charm quark mass just reduces from  $m_c = 1.35$  GeV to 1.34 GeV. The only parameter which  $m_c$  is sensitive to is the effective gluon mass  $m_g$ : a smaller (larger)  $m_g = 0.40$  GeV (0.42 GeV) gives  $m_c = 1.29$  GeV (1.40 GeV). This sensitivity is expected, for the hadronic threshold  $m_F$ , which the Wilson coefficients can evolve to, is quite low in this case. It is then understood why we chose  $m_g = 0.41$  GeV: the resultant  $D^+$  meson mass  $m_{D^+} = 1.85$  GeV would be roughly equal to the observed one. We point out that the  $Q \rightarrow d\bar{u}d$  decay is the only mode among those considered in the present work, whose analysis is sensitive to  $m_g$ . Once  $m_g$  is set, it is employed in the investigations of the other modes, and the agreement of the solved fermion masses with the measured values will reinforce our claim that fermion masses in the SM are dynamically constrained.

We also need to assess the theoretical uncertainty inherent in our formalism. Though the large  $N$  approximations for establishing a solution are justified, it is not clear how large the highest degree  $N'$  in Eq. (21) is and how reliable the expression in terms of a single Bessel function in Eq. (26) is. This uncertainty is reflected by that of the parameter  $\bar{\omega}$  from matching the solution to the HQE input in the interval  $(0, m_F)$ —if a true solution was available,  $\bar{\omega}$  should be determined unambiguously. Different ways of matching return different values of  $\bar{\omega}$ , as having been exemplified below Eq. (33), and different results of  $m_c$  accordingly. We estimate the error from this source by computing the squared deviation

$$\sigma \equiv \int_0^{m_F} \left[ \Delta\Gamma_h(m_Q)|_{\omega=\bar{\omega}} + \Gamma_h^{\text{HQE}}(m_Q) \right]^2 dm_Q. \quad (36)$$

A value of  $\bar{\omega}$  is accepted, as  $\sigma$  is lower than twice its minimum, which corresponds to the best fit. Given this prescription, it is straightforward to identify the allowed ranges  $3.012 \text{ GeV}^{-1} < \bar{\omega} < 3.306 \text{ GeV}^{-1}$  and  $1.29 \text{ GeV} < m_c < 1.41 \text{ GeV}$ . Since the effective gluon mass will be fixed hereafter, the uncertainties surveyed above are

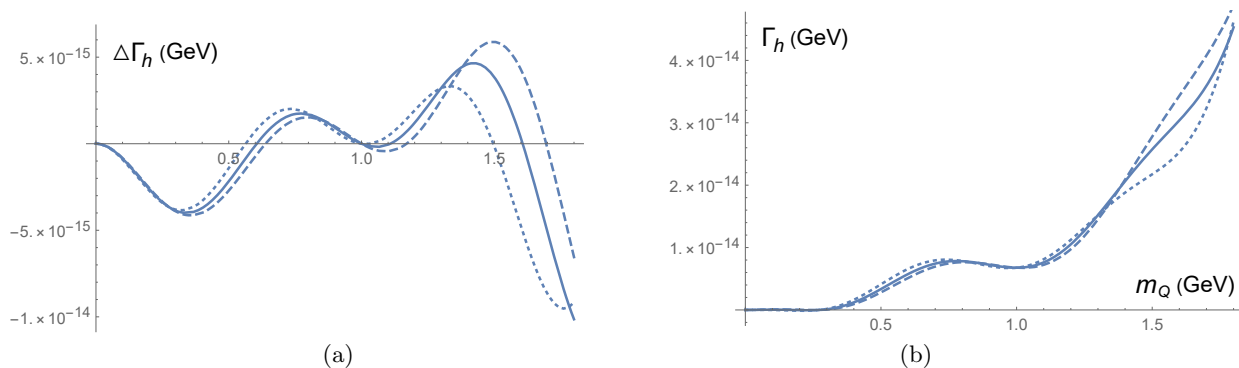


FIG. 5: Dependencies of (a) the subtracted width  $\Delta\Gamma_h(m_Q)$  and (b) the width  $\Gamma_h(m_Q)$  of the  $Q \rightarrow dud\bar{d}$  decay on  $m_Q$  for  $\omega = 3.0 \text{ GeV}^{-1}$  (dashed line),  $3.166 \text{ GeV}^{-1}$  (solid line) and  $3.4 \text{ GeV}^{-1}$  (dotted line).

dominated by the variation of  $\bar{\omega}$ , and sum to  $m_c = 1.35^{+0.07}_{-0.06} \text{ GeV}$ .

We then include the CKM factor  $|V_{\text{CKM}}|^2 = |V_{cd}V_{ud}^*|^2$  with  $V_{cd} = \lambda$  and  $V_{ud} = 1 - \lambda^2/2$ , where the Wolfenstein parameter takes  $\lambda = 0.225$  [55]. The subtracted width  $\Delta\Gamma_h(m_Q)$  and the width  $\Gamma_h(m_Q) = \Delta\Gamma_h(m_Q) + \Gamma_h^{\text{HQE}}(m_Q)$  of the  $Q \rightarrow dud\bar{d}$  decay for three values of  $\omega$  around  $\bar{\omega} = 3.166 \text{ GeV}^{-1}$ , i.e., for  $\omega = 3.0 \text{ GeV}^{-1}$ ,  $3.166 \text{ GeV}^{-1}$  and  $3.4 \text{ GeV}^{-1}$  are plotted in Figs. 5(a) and 5(b). Indeed all three curves cross each other in the compact regions located at  $m_Q = 0.84 \text{ GeV}$  and  $1.35 \text{ GeV}$  as expected, evincing the stability of the widths evaluated at these two values of  $m_Q$  under the variation of  $\omega$ . The intersection area is smaller at  $m_Q = 0.84 \text{ GeV}$  than at  $m_Q = 1.35 \text{ GeV}$ , in alignment with the indication of the second derivative in Fig. 4. However, we pick up the latter as the solution for the charm quark mass as explained before. It is mentioned that the similar phenomenon has occurred in the dispersive analysis of neutral meson mixing; the curves for the mixing parameters of a fictitious  $D$  meson corresponding to various scales  $\Lambda$  also cross each other in a compact region located at the  $D$  meson mass. We clarify that the crossing at  $m_Q = 1 \text{ GeV}$ , also seen in Fig. 5, is due to the vanishing of the factor  $1 - m_Q/(2\Lambda)$  in Eq. (33), which should not be mixed up with the roots of Eq. (34). The diminishing of the solved  $\Gamma_h(m_Q)$  for small  $m_Q$  up to  $m_Q = m_F = 0.275 \text{ GeV}$  in Fig. 5(b) echoes the almost exact cancellation between  $\Delta\Gamma_h(m_Q)$  and  $\Gamma_h^{\text{HQE}}(m_Q)$  in the interval  $(0, m_F)$ , which has been illustrated in Fig. 3.

The predicted widths at  $m_Q = m_c = 1.35 \text{ GeV}$  read  $\Delta\Gamma_h(m_c) = 4.09 \times 10^{-15} \text{ GeV}$  and  $\Gamma_h(m_c) = 1.79 \times 10^{-14} \text{ GeV}$ . It signifies that the nonperturbative effect, originating from the introduction of the hadronic threshold, enhances the HQE result by about 30%. The predicted hadronic decay width amounts to the branching fraction  $B(c \rightarrow dud\bar{d}) = 2.8\%$  for the inclusive Cabibbo-suppressed pionic modes, given the total decay width of the  $D^+$  meson  $\Gamma^{\text{tot}} = 6.37 \times 10^{-13} \text{ GeV}$  [55]. This prediction is reasonable compared with the relevant data [55]. The decay width  $\Gamma_h(0.84 \text{ GeV}) = 7.66 \times 10^{-15} \text{ GeV}$  at  $m_Q = 0.84 \text{ GeV}$ , amounting to the branching fraction 1.2%, is apparently too low; the single channel  $D^+ \rightarrow 2\pi^+\pi^-\pi^0$  contributes the branching fraction about 1.2% already according to [55].

### III. DISPERSIVE CONSTRAINTS ON OTHER FERMION MASSES

We extend the formalism developed in the previous section to the constraints on the other fermion masses, including the strange quark mass  $m_s$  from the  $Q \rightarrow sud\bar{d}$  decay, the bottom quark mass  $m_b$  from the  $Q \rightarrow c\bar{u}d$  decay, the muon mass  $m_\mu$  from the  $Q \rightarrow d\mu^+\nu_\mu$  decay and the  $\tau$  lepton mass  $m_\tau$  from the  $Q \rightarrow u\tau^-\bar{\nu}_\tau$  decay. For the constraints on  $m_s$ ,  $m_\mu$  and  $m_\tau$ , we rely on the proposition that dispersive analyses of different decay channels of a fictitious heavy quark should conclude the same heavy quark mass.

#### A. The $Q \rightarrow sud\bar{d}$ and $Q \rightarrow c\bar{u}d$ Decays

We first derive a solution to the dispersion relation obeyed by hadronic decay widths for massive final states, e.g., with nonvanishing  $m_q$  in Eq. (7). Similarly, we decompose the HQE input into the sum of the even and odd pieces  $\Gamma_h^{\text{HQE}}(m) = \Gamma_e^{\text{HQE}}(m) + \Gamma_o^{\text{HQE}}(m)$ , and the unknown width into  $\Gamma_h(m) = \Gamma_e(m) + \Gamma_o(m)$ . Note that there exists an

additional pole at  $m_Q = 0$  in the HQE result as shown in Eq. (7),

$$\Gamma_h^{(6)+(7)}(m_Q) \propto \frac{(m_Q^2 - m_q^2)^2}{m_Q} - 4\bar{\Lambda}(m_Q^2 - m_q^2), \quad (37)$$

where the expansion of the factor  $1 + m_q^2/m_Q^2 \approx 2 + O((m_Q^2 - m_q^2)/m_Q^2)$  in the limit  $m_Q \rightarrow m_q$  has been applied to the second term. The single pole in the dimension-six term requests a slightly different handling as elaborated below. The dispersion relation for the even piece is similar to Eq. (14), except that the lower bound of  $m^2$  is replaced by the quark-level threshold  $m_q^2$ ,

$$\int_{m_q^2}^{\infty} \frac{\Delta\Gamma_e(m)}{m_Q^2 - m^2} dm^2 = 0. \quad (38)$$

The unknown function  $\Delta\Gamma_e(m)$  is fixed to  $-\Gamma_e^{\text{HQE}}(m)$  in the interval  $(m_q, m_F)$  of  $m$  with the hadronic threshold  $m_F$ .

For the odd piece, we consider the contour integration of the correlator  $m^2\Pi(m)/(m^2 - m_q^2)$ , for which the high-mass behavior of  $\Pi(m)$  is not altered, and the  $m = 0$  pole has been removed, so that Eq. (9) holds. The additional poles at  $m = \pm m_q$  are introduced, but their contribution  $m_q M(m_q)/m_Q$  to the left-hand side of Eq. (10) is much smaller than  $M(m_Q)$  from the pole  $m = m_Q$  at large  $m_Q$ . A similar contribution from the poles at  $m = \pm m_q$  also exists on the left-hand side of Eq. (11). We still equate the left-hand sides of Eqs. (10) and (11), and this equality is justified, as long as the odd piece  $m^2\Gamma_o(m)/(m^2 - m_q^2)$  can be solved from the dispersion relation

$$\begin{aligned} & \int_{m_F}^R \frac{m^2\Gamma_o(m)}{(m^2 - m_q^2)(m_Q - m)} dm - \int_{-R}^{-m_F} \frac{m^2\Gamma_o(m)}{(m^2 - m_q^2)(m_Q - m)} dm \\ &= \int_{m_q}^R \frac{m^2\Gamma_o^{\text{HQE}}(m)}{(m^2 - m_q^2)(m_Q - m)} dm - \int_{-R}^{-m_q} \frac{m^2\Gamma_o^{\text{HQE}}(m)}{(m^2 - m_q^2)(m_Q - m)} dm. \end{aligned} \quad (39)$$

Employing the variable change  $m \rightarrow -m$  for the second integrals on both sides and moving the integrands on the right-hand side to the left-hand side, we get

$$\int_{m_q^2}^{\infty} \frac{m\Delta\Gamma_o(m)}{(m^2 - m_q^2)(m_Q^2 - m^2)} dm^2 = 0, \quad (40)$$

where the upper bound of the integration variable  $m^2$  has been extended to infinity. The unknown function  $\Delta\Gamma_o(m)$  is fixed to  $-\Gamma_o^{\text{HQE}}(m)$  in the interval  $(m_q, m_F)$ .

The steps from Eq. (17) to Eq. (25) can be carried out for the current case with massive final states straightforwardly. The only modification resides in the variable changes  $m_Q^2 - m_q^2 = u\Lambda$  and  $m^2 - m_q^2 = v\Lambda$ . We then construct the solutions

$$\Delta\Gamma_e(m) \approx y_e \left( \omega \sqrt{m^2 - m_q^2} \right)^\alpha J_\alpha \left( 2\omega \sqrt{m^2 - m_q^2} \right), \quad (41)$$

$$\frac{m\Delta\Gamma_o(m)}{m^2 - m_q^2} \approx y_o \left( \omega \sqrt{m^2 - m_q^2} \right)^\alpha J_\alpha \left( 2\omega \sqrt{m^2 - m_q^2} \right). \quad (42)$$

A solution of the hadronic decay width is written as

$$\Delta\Gamma_h(m_Q) = \Delta\Gamma_e(m_Q) + \Delta\Gamma_o(m_Q) \approx y_e \left( 1 + \frac{y_o}{y_e} \frac{m_Q^2 - m_q^2}{m_Q} \right) \left( \omega \sqrt{m_Q^2 - m_q^2} \right)^\alpha J_\alpha \left( 2\omega \sqrt{m_Q^2 - m_q^2} \right), \quad (43)$$

which reduces to Eq. (26) as  $m_q = 0$  obviously.

We apply Eq. (43) to the channel  $Q \rightarrow s\bar{u}d$  with the thresholds  $m_q = m_s$  and  $m_F = m_{\pi^+} + m_{\bar{K}^0}$ . Comparing Eqs. (43) and (37) in the limit  $m_Q \rightarrow m_q$ , we identify the index  $\alpha = 1$  and the ratio

$$\frac{y_o}{y_e} = -\frac{1}{4\Lambda} = -0.5 \text{ GeV}^{-1}. \quad (44)$$

The boundary condition  $\Delta\Gamma_h(m_F) = -\Gamma_h^{\text{HQE}}(m_F)$  at  $m_Q = m_F$  leads Eq. (43) to

$$\Delta\Gamma_h(m_Q) = -\Gamma_h^{\text{HQE}}(m_F) \left( 1 - \frac{m_Q^2 - m_s^2}{4\Lambda m_Q} \right) \left( 1 - \frac{m_F^2 - m_s^2}{4\Lambda m_Q} \right)^{-1} \frac{\sqrt{m_Q^2 - m_s^2} J_1 \left( 2\omega \sqrt{m_Q^2 - m_s^2} \right)}{\sqrt{m_F^2 - m_s^2} J_1 \left( 2\omega \sqrt{m_F^2 - m_s^2} \right)}. \quad (45)$$

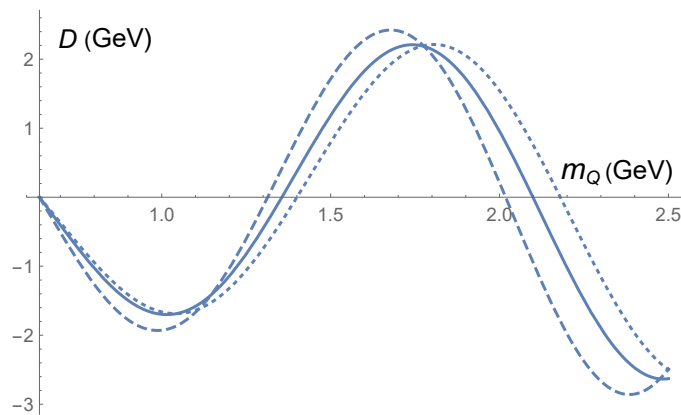


FIG. 6: Dependencies of  $D(m_Q)$  in Eq. (46) on  $m_Q$  for  $m_s = 0.01$  GeV (dotted line),  $0.12$  GeV (solid line) and  $0.30$  GeV (dashed line).

With the same binding energy  $\bar{\Lambda} = 0.5$  GeV and effective gluon mass  $m_g = 0.41$  GeV, and the meson masses  $m_{\pi^+} = 0.140$  GeV and  $m_{\bar{K}^0} = 0.498$  GeV, we obtain  $\bar{\omega} = 1.995$  GeV $^{-1}$ ,  $2.080$  GeV $^{-1}$  and  $2.177$  GeV $^{-1}$  for the strange quark mass  $m_s = 0.01$  GeV,  $0.12$  GeV and  $0.30$  GeV, respectively, from the best fit of Eq. (45) to  $-\Gamma_h^{\text{HQE}}(m_Q)$  in the interval  $(m_s, m_F)$ .

The stability of the solved decay width under the variation of  $\omega$  demands the vanishing of the derivative  $d\Delta\Gamma_h(m_Q)/d\omega$  at  $\omega = \bar{\omega}$ , i.e.,

$$D(m_Q) \equiv \left. \frac{d}{d\omega} \frac{J_1\left(2\omega\sqrt{m_Q^2 - m_s^2}\right)}{J_1\left(2\omega\sqrt{m_F^2 - m_s^2}\right)} \right|_{\omega=\bar{\omega}} = 0. \quad (46)$$

The dependencies of the above derivative on  $m_Q$  for the three values of  $\bar{\omega}$  are exhibited in Fig. 6, where the first roots located at  $m_Q = m_F$  have no physical significance, because they arise from the boundary condition. We read off the second roots  $m_Q = 1.40$  GeV,  $1.35$  GeV and  $1.31$  GeV for  $\bar{\omega} = 1.995$  GeV $^{-1}$ ,  $2.080$  GeV $^{-1}$  and  $2.177$  GeV $^{-1}$  ( $m_s = 0.01$  GeV,  $0.12$  GeV and  $0.30$  GeV), respectively, at which the solutions possess the maximal stability as argued in the previous section. Those roots at higher  $m_Q$  with worse stability are not selected. It is encouraging to find that the strange quark must have a mass around  $m_s = 0.12$  GeV in order to maintain the charm quark mass  $m_c = 1.35$  GeV, the same as from the  $Q \rightarrow du\bar{d}$  analysis. A lower (higher)  $m_s$  would give rise to a higher (lower)  $m_c$ . We have also checked that it is impossible to reproduce the charm quark mass without the spectator contribution in Eq. (37);  $m_c$  is always higher than  $3.0$  GeV for any  $m_s < m_K$ , once the spectator contribution is switched off. That is, the higher-power effect is necessary for establishing the physical solution.

The result  $m_s = 0.12$  GeV is consistent with the one derived from the known kaon mass  $m_K$  in QCD sum rules at the scale  $\mu = m_c = 1.35$  GeV [22]. The above observation confirms the nontrivial correlation among the masses  $m_s$ ,  $m_\pi$ ,  $m_K$  and  $m_c$ , which characterize strong and weak dynamics in the SM, though their exact values may suffer potential theoretical uncertainties from, say, higher-order corrections to the HQE input. It is verified that the extractions from the  $Q \rightarrow su\bar{d}$  decay width are less sensitive to the variation of the effective gluon mass  $m_g$ . It can take a value as low (high) as  $0.35$  GeV ( $0.46$  GeV) to decrease (increase)  $m_c$  to  $1.30$  GeV ( $1.40$  GeV) for  $m_s = 0.12$  GeV. In the previous  $Q \rightarrow du\bar{d}$  case,  $m_g$  takes  $0.40$  GeV ( $0.42$  GeV) to make the same amount of impact to the solution of  $m_c$ . The influence from the other parameters, like the HQET ones, is also milder. To estimate the uncertainty from the variation of  $\bar{\omega}$ , we search for its value for each  $m_s$ , which generates  $m_c = 1.35$  GeV from Eq. (46). It is then examined whether the squared deviation for this set of  $\bar{\omega}$  and  $m_s$ , defined similarly to Eq. (36) but with the integration interval  $(m_s, m_F)$ , is below twice its minimum. If it is, the considered  $m_s$  value is accepted. Iterating the procedure for various  $m_s$ , we can acquire the allowed range of  $m_s$  in principle. It turns out that the resultant range  $m_s < 0.4$  GeV is very wide. On one hand, the above error estimate may be too conservative to achieve effective bounds in this case. On the other hand, it discloses the worse quality of the solution compared to that for the  $Q \rightarrow du\bar{d}$  decay. The worse quality could be attributed to the more complicated functional form of the HQE input for massive final states than for massless ones, such that the simple solution in Eq. (45) is less accurate than in Eq. (26). Therefore, we do not attach errors to the determination of  $m_s$ .

The  $m_Q$  dependencies of the subtracted width  $\Delta\Gamma_h(m_Q)$  in Eq. (45) and the width  $\Gamma_h(m_Q)$  of the  $Q \rightarrow su\bar{d}$  decay for three values of  $\omega$  around  $\bar{\omega}$  from the best fit, i.e.,  $\omega = 1.9$  GeV $^{-1}$ ,  $2.080$  GeV $^{-1}$  and  $2.3$  GeV $^{-1}$ , are

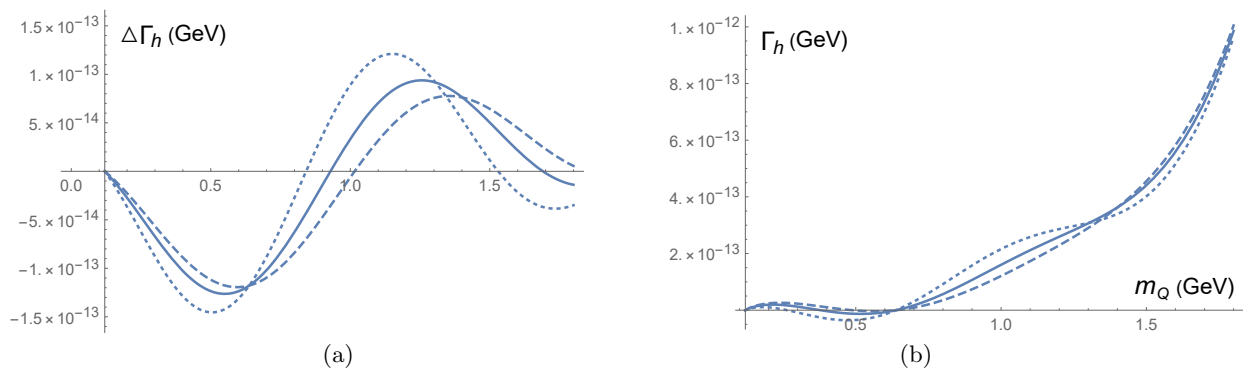


FIG. 7: Dependencies of (a) the subtracted width  $\Delta\Gamma_h(m_Q)$  and (b) the width  $\Gamma_h(m_Q)$  of the  $Q \rightarrow sud\bar{}$  decay on  $m_Q$  for  $\omega = 1.9 \text{ GeV}^{-1}$  (dashed line),  $2.080 \text{ GeV}^{-1}$  (solid line) and  $2.3 \text{ GeV}^{-1}$  (dotted line).

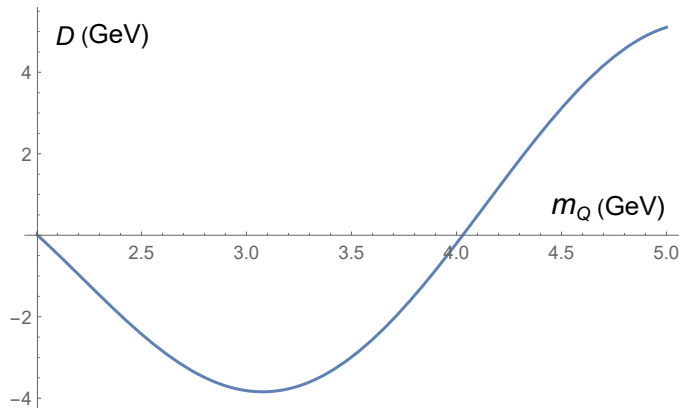


FIG. 8: Dependencies of  $D(m_Q)$  in Eq. (46) on  $m_Q$  for the  $Q \rightarrow cud\bar{}$  decay.

plotted in Figs. 7(a) and 7(b), respectively, where the CKM factor  $|V_{\text{CKM}}|^2 = |V_{cs}V_{ud}^*|^2$  has been included with  $V_{cs} = 1 - \lambda^2/2$ . The small  $\Gamma_h(m_Q)$  in the interval  $(m_s, m_F)$  of  $m_Q$  with  $m_s = 0.12 \text{ GeV}$  and  $m_F = 0.638 \text{ GeV}$  in Fig. 7(b) reflects the satisfactory match between  $\Delta\Gamma_h(m_Q)$  and  $-\Gamma_h^{\text{HQE}}(m_Q)$ . The three curves cross each other more tightly at  $m_Q = 1.35 \text{ GeV}$ , implying the stability of the widths at this  $m_Q$  under the variation of  $\omega$ . The crossing occurring at  $m_Q = m_F = 0.638 \text{ GeV}$ , due to the boundary condition, bears no physical significance. The predicted widths  $\Delta\Gamma_h(m_c) = 8.61 \times 10^{-14} \text{ GeV}$  and  $\Gamma_h(m_c) = 3.33 \times 10^{-13} \text{ GeV}$  at  $m_c = 1.35 \text{ GeV}$  can be read off easily. It indicates that the nonperturbative effect, originating from the introduction of the hadronic threshold, enhances the HQE result by about 35%. The above decay width amounts to the branching fraction  $B(c \rightarrow sud\bar{}) = 52.3\%$  for the inclusive Cabibbo-favored modes. Since the branching fraction of the semileptonic  $D^+$  meson decays is about 34% [55], and the Cabibbo-favored modes dominate the hadronic channel, our prediction is reasonable. Thanks to the nonperturbative enhancement observed in our formalism, the charmed meson lifetimes can be accommodated without resorting to a large fitted charm quark mass  $1.56 \text{ GeV}$  [24].

We turn to the analysis of the  $Q \rightarrow c\bar{u}d$  decay width, simply substituting  $m_c$  for the final-state quark mass  $m_s$  and  $m_F = m_{\pi^+} + m_{D^0}$  for the threshold  $m_F = m_{\pi^+} + m_{\bar{K}^0}$ . Another modification occurs in the choice of the QCD scale  $\Lambda_{\text{QCD}} = 0.286 \text{ GeV}$  for the active quark number  $n_f = 4$  [52]. Taking the same binding energy  $\bar{\Lambda} = 0.5 \text{ GeV}$  and effective gluon mass  $m_g = 0.41 \text{ GeV}$ ,  $m_c = 1.35 \text{ GeV}$  extracted previously and  $m_{D^0} = 1.865 \text{ GeV}$  [55], we derive  $\bar{\omega} = 0.712 \text{ GeV}^{-1}$  from the best fit of the solution in Eq. (45) to the constraint  $-\Gamma_h^{\text{HQE}}(m_Q)$  in the interval  $(m_c, m_F)$ . Figure 8 shows the dependence of the derivative in Eq. (46) on  $m_Q$ , and the second root located at  $m_Q = 4.03 \text{ GeV}$  corresponds to the physical bottom quark mass  $m_b$ , close to the running quark mass  $\bar{m}_b(\bar{m}_b) = 4.248 \text{ GeV}$  [24]. We stress that the formula for  $\Gamma_h^{\text{HQE}}(m_Q)$  does not carry any a priori information on a bottom quark, the emergence of  $m_b$  is nontrivial, and the dispersion relation correlates the masses  $m_c$ ,  $m_D$  and  $m_b$ . This correlation is solid in the sense that it is not affected by the variation of  $m_g$ , because of the sizable threshold  $m_F$ . For instance,  $\pm 25\%$  change of  $m_g$  induces only  $\pm 0.5\%$  change of  $m_b$ . We simply concentrate on the theoretical error inherent in our formalism.

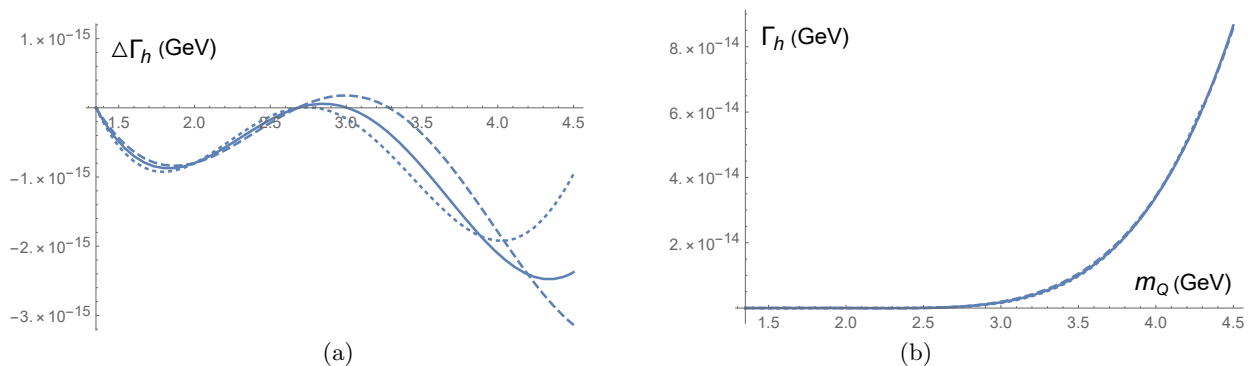


FIG. 9: Dependencies of (a) the subtracted width  $\Delta\Gamma_h(m_Q)$  and (b) the width  $\Gamma_h(m_Q)$  of the  $Q \rightarrow c\bar{u}d$  decay on  $m_Q$  for  $\omega = 0.64$  GeV $^{-1}$  (dashed line),  $0.712$  GeV $^{-1}$  (solid line) and  $0.78$  GeV $^{-1}$  (dotted line).

The condition that the squared deviation, defined similarly to Eq. (36), does not exceed twice its minimum leads to the allowed range  $0.706$  GeV $^{-1} < \bar{\omega} < 0.718$  GeV $^{-1}$ . We thus get the range of the bottom quark mass  $4.01$  GeV  $< m_b < 4.06$  GeV, and conclude  $m_b = 4.03_{-0.02}^{+0.03}$  GeV.

One may wonder that the predicted  $B$  meson mass  $m_B = m_b + \bar{\Lambda} = 4.53$  is lower than the measured value  $5.279$  GeV [55]. It may be due to the same HQET input  $\bar{\Lambda} = 0.5$  GeV assumed in the analyses of the  $D$  and  $B$  meson decays. In fact, the binding energy  $\bar{\Lambda}$  can be  $m_Q$ -dependent as mentioned before. If  $\bar{\Lambda}(m_Q)$  increases with  $m_Q$ , we will be allowed to test a larger value, say,  $\bar{\Lambda} = 0.6$  GeV for the  $Q \rightarrow c\bar{u}d$  decay, which yields  $m_b = 4.42$  GeV. It lifts the predicted  $B$  meson mass up to  $5.02$  GeV, approaching the observed one.

We present the dependencies of the subtracted width  $\Delta\Gamma_h(m_Q)$  and the width  $\Gamma_h(m_Q)$  of the  $Q \rightarrow c\bar{u}d$  decay with three different  $\omega$  values in Figs. 9(a) and 9(b), respectively, where the CKM factor  $|V_{\text{CKM}}|^2 = |V_{cb}V_{ud}^*|^2$  has been included with  $V_{cb} = A\lambda^2/2$ ,  $A = 0.826$  being one of the Wolfenstein parameters [55]. It is noticed that the three curves corresponding to  $\omega = 0.64$  GeV $^{-1}$ ,  $0.712$  GeV $^{-1}$  and  $0.78$  GeV $^{-1}$  cross each other in the small region located at  $m_Q \approx 4$  GeV in Fig. 9(a). The crossings at  $m_Q = m_F = 2.005$  GeV resulting from the boundary condition, and at  $m_Q = 2.680$  which vanishes the factor  $1 - (m_Q^2 - m_c^2)/(4\bar{\Lambda}m_Q)$  in Eq. (45), have no physical significance. The three curves are on top of one another in Fig. 9(b), and their intersection is barely seen, for the magnitude of  $\Delta\Gamma_h(m_Q)$  is much lower than  $\Gamma_h(m_Q)$ . The smallness of  $\Delta\Gamma_h(m_Q)$  reveals a minor nonperturbative contribution to  $B$  meson decays introduced by the hadronic threshold  $m_F$ , and explains the reliability of HQE for the evaluation of  $B$  meson lifetimes. The solved  $\Gamma_h(m_Q)$  remains vanishing in the interval  $(m_c, m_F)$  of  $m_Q$  (in fact, up to  $m_Q = 2.5$  GeV) in Fig. 9(b), manifesting the perfect match between  $\Delta\Gamma_h(m_Q)$  and  $-\Gamma_h^{\text{HQE}}(m_Q)$ . We read off the widths  $\Delta\Gamma_h(m_b) = -2.16 \times 10^{-15}$  GeV and  $\Gamma_h(m_b) = 3.61 \times 10^{-14}$  GeV, which amounts to the branching fraction  $B(b \rightarrow c\bar{u}d) = 9.0\%$ , given the total decay width of the  $B^\pm$  meson  $\Gamma^{\text{tot}} = 4.02 \times 10^{-13}$  GeV [55]. The dominant percent-level branching fractions of  $B^+$  meson decays,  $0.47\%$  from  $\bar{D}^0\pi^+$ ,  $1.34\%$  from  $\bar{D}^0\rho^+$ ,  $0.41\%$  from  $\bar{D}^0\omega\pi^+$ ,  $0.56\%$  from  $\bar{D}^0\pi^+\pi^+\pi^-$ ,  $0.52\%$  from  $\bar{D}^*(2007)^0\pi^+$ ,  $0.98\%$  from  $\bar{D}^*(2007)^0\rho^+$ ,  $0.45\%$  from  $\bar{D}^*(2007)^0\omega\pi^+$ ,  $1.03\%$  from  $\bar{D}^*(2007)^0\pi^+\pi^+\pi^-$ ,  $1.8\%$  from  $\bar{D}^*(2007)^0\pi^-\pi^+\pi^+\pi^0$ ,  $0.57\%$  from  $\bar{D}^{*0}3\pi^+2\pi^-$  and  $0.57\%$  from  $\bar{D}^{*0}\pi^+$  [55], add up to  $8.7\%$ , in agreement with our prediction.

A remark is in order. A bottom quark can also decay into light quarks through the  $Q \rightarrow u\bar{u}d$  channel. It has been found that the dispersion relation for a fictitious heavy quark  $Q$  decay into light final states determines only the charm quark mass. The larger bottom quark mass, even if it appears as one of the roots that vanishes the first derivative with respect to  $\omega$ , will not be selected due to the worse associated stability. In other words, the  $Q \rightarrow u\bar{u}d$  mode is not efficient for the constraint of the bottom quark mass. We have elucidated in Sec. II that an appropriate correlation function needs to be chosen for the purpose. For example, the  $D^0$  meson decay width does not work for the determination of the charm quark mass owing to the chirally suppressed dimension-six contribution. This guideline also applies to analyses in lattice QCD and sum rules, which require suitable correlation functions for extractions of physical observables.

### B. The $Q \rightarrow d\mu^+\nu_\mu$ and $Q \rightarrow u\tau^-\bar{\nu}_\tau$ Decays

The investigations on semileptonic and hadronic decay widths should return the same heavy quark mass from the viewpoint of the dynamical consistency, so the dispersion relations for the former can be utilized to constrain lepton masses. The weak annihilation contribution in semileptonic decays plays a role similar to the Pauli interference effect in hadronic decays for establishing a solution. Because the  $e\nu_e$  channel with a tiny electron mass contains a negligible

annihilation contribution, which does not provide a sufficient power correction, the  $\mu\nu_\mu$  and  $\tau\nu_\tau$  channels will be studied here. Equation (8) is proportional, in the limit  $m_Q \rightarrow m_\ell$ , to

$$\Gamma_s^{(6)+(7)}(m_Q) \propto \frac{3}{2} \frac{(m_Q^2 - m_\ell^2)^2 m_\ell^2}{m_Q^3} + 6\bar{\Lambda} \frac{(m_Q^2 - m_\ell^2) m_\ell^2}{m_Q^2}, \quad (47)$$

where the expansion  $m_{H_Q} = m_Q + \bar{\Lambda}$  has been inserted and the net dimension-seven contribution has been approximated by  $3 - 7m_\ell^2/m_Q^2 \approx -4 + O((m_Q^2 - m_\ell^2)/m_Q^2)$  to give the second term. It is evident that the above expression follows the aforementioned helicity suppression; namely, the weak annihilation contribution diminishes with a lepton mass. A feature different from hadronic widths is that the dimension-six contribution is constructive in the present case, and the dimension-seven contribution is destructive. It turns out that the  $Q \rightarrow d\mu^+\nu_\mu$  decay width becomes negative in the low  $m_Q$  region, though it is positive at  $m_Q = m_c$ , and some adjustment of the HQE input is necessary for solving the dispersion relation. Therefore, we discuss the  $Q \rightarrow u\tau^-\bar{\nu}_\tau$  decay first, whose width remains positive in the whole range of  $m_Q$ .

As indicated in Eq. (47), both the even piece  $\Gamma_e^{\text{HQE}}(m)$  and the odd piece  $\Gamma_o^{\text{HQE}}(m)$  have poles at  $m = 0$ . For the even piece, we consider the contour integration of the correlator  $m^2\Pi(m)/(m^2 - m_\tau^2)$  with the perturbative threshold  $m_\tau$ . The high-mass behavior stays the same, and the  $m = 0$  pole has been removed, so that Eq. (9) holds. The similar procedure applied to Eq. (39) yields

$$\int_{m_\tau^2}^{\infty} \frac{m^2 \Delta\Gamma_e(m)}{(m^2 - m_\tau^2)(m_Q^2 - m^2)} dm^2 = 0, \quad (48)$$

where the unknown function  $\Delta\Gamma_e(m)$  is fixed to  $-\Gamma_e^{\text{HQE}}(m)$  in the interval  $(m_\tau, m_F)$  (a neutrino is regarded as being massless) with the physical threshold  $m_F = m_{\pi^0} + m_\tau$ . For the odd piece, we consider the contour integration of the correlator  $m^4\Pi(m)/(m^2 - m_\tau^2)^2$  to remove the triple pole at  $m = 0$ , and derive the dispersion relation

$$\begin{aligned} & \int_{m_F}^R \frac{m^4 \Gamma_e(m)}{(m^2 - m_\tau^2)^2 (m_Q - m)} dm - \int_{-R}^{-m_F} \frac{m^4 \Gamma_e(m)}{(m^2 - m_\tau^2)^2 (m_Q - m)} dm \\ &= \int_{m_\tau}^R \frac{m^4 \Gamma_e^{\text{HQE}}(m)}{(m^2 - m_\tau^2)^2 (m_Q - m)} dm - \int_{-R}^{-m_\tau} \frac{m^4 \Gamma_e^{\text{HQE}}(m)}{(m^2 - m_\tau^2)^2 (m_Q - m)} dm. \end{aligned} \quad (49)$$

We then have, with the variable change  $m \rightarrow -m$  for the second integrals on both sides,

$$\int_{m_\tau^2}^{\infty} \frac{m^3 \Delta\Gamma_o(m)}{(m^2 - m_\tau^2)^2 (m_Q^2 - m^2)} dm^2 = 0, \quad (50)$$

where the upper bound of the integration variable  $m^2$  has been pushed to infinity. The unknown function  $\Delta\Gamma_o(m)$  is fixed to  $-\Gamma_o^{\text{HQE}}(m)$  in the interval  $(m_\tau, m_F)$ .

The solutions from Eqs. (48) and (50) are written as

$$\frac{m^2 \Delta\Gamma_e(m)}{m^2 - m_\tau^2} \approx y_e \left( \omega \sqrt{m^2 - m_\tau^2} \right)^\alpha J_\alpha \left( 2\omega \sqrt{m^2 - m_\tau^2} \right), \quad (51)$$

$$\frac{m^3 \Delta\Gamma_o(m)}{(m^2 - m_\tau^2)^2} \approx y_o \left( \omega \sqrt{m^2 - m_\tau^2} \right)^\alpha J_\alpha \left( 2\omega \sqrt{m^2 - m_\tau^2} \right), \quad (52)$$

respectively, whose combination gives the subtracted width of the  $Q \rightarrow u\tau^-\bar{\nu}_\tau$  decay

$$\Delta\Gamma_s(m_Q) \approx y_e \left( 1 + \frac{y_o}{y_e} \frac{m_Q^2 - m_\tau^2}{m_Q} \right) \frac{m_Q^2 - m_\tau^2}{m_Q^2} \left( \omega \sqrt{m_Q^2 - m_\tau^2} \right)^\alpha J_\alpha \left( 2\omega \sqrt{m_Q^2 - m_\tau^2} \right). \quad (53)$$

Comparing the behaviors of Eqs. (47) and (53) in the limit  $m_Q \rightarrow m_\tau$ , we set the index  $\alpha = 0$  and the ratio

$$\frac{y_o}{y_e} = \frac{1}{4\bar{\Lambda}} = 0.5 \text{ GeV}^{-1}. \quad (54)$$

The boundary condition  $\Delta\Gamma_s(m_F) = -\Gamma_s^{\text{HQE}}(m_F)$  at  $m_Q = m_F$  fixes the overall coefficient

$$y_e = -\Gamma_s^{\text{HQE}}(m_F) \left[ \left( 1 + \frac{m_F^2 - m_\tau^2}{4\bar{\Lambda}m_F} \right) \frac{(m_F^2 - m_\tau^2)}{m_F^2} J_0 \left( 2\omega \sqrt{m_F^2 - m_\tau^2} \right) \right]^{-1}. \quad (55)$$



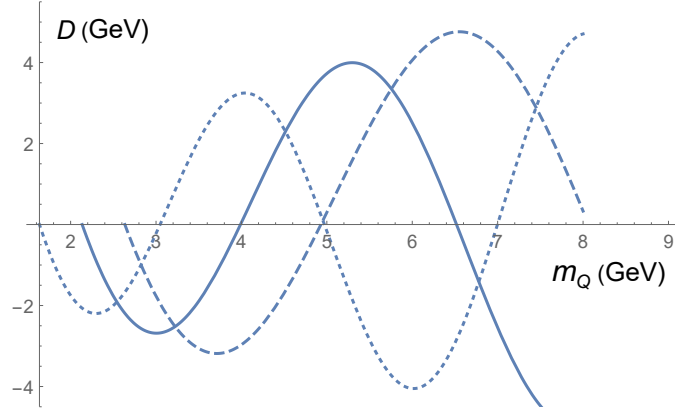


FIG. 10: Dependencies of  $D(m_Q)$  in Eq. (56) on  $m_Q$  for  $m_\tau = 1.5$  GeV (dotted line), 2.0 GeV (solid line) and 2.5 GeV (dashed line).

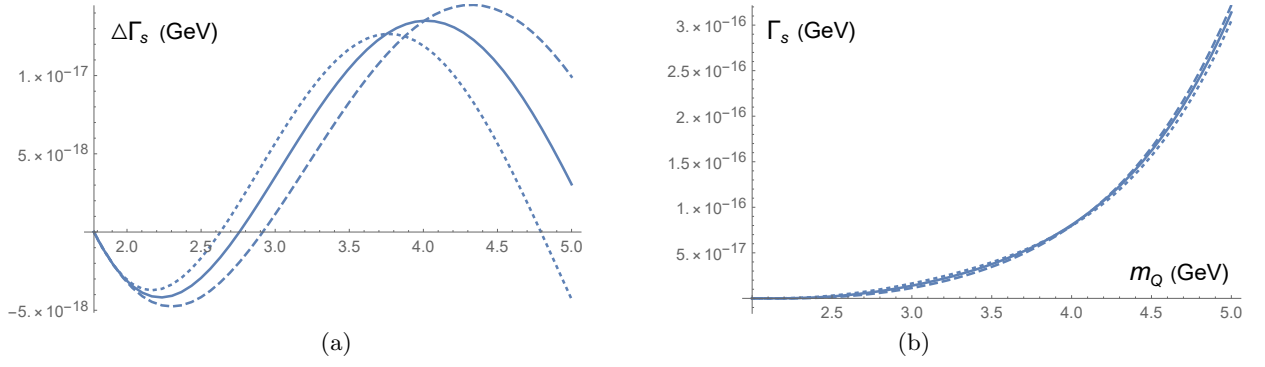


FIG. 11: Dependencies of (a) the subtracted width  $\Delta\Gamma_s(m_Q)$  and (b) the width  $\Gamma_s(m_Q)$  of the  $Q \rightarrow u\tau^-\bar{\nu}_\tau$  decay on  $m_Q$  for  $\omega = 0.52$   $\text{GeV}^{-1}$  (dashed line),  $0.570$   $\text{GeV}^{-1}$  (solid line) and  $0.62$   $\text{GeV}^{-1}$  (dotted line).

The parameter  $\bar{\omega}$  is obtained from the best fit of Eq. (53) to  $-\Gamma_s^{\text{HQE}}(m_Q)$  in the interval  $(m_\tau, m_F)$  with the same binding energy  $\bar{\Lambda} = 0.5$  GeV. We get  $\bar{\omega} = 0.748$   $\text{GeV}^{-1}$ ,  $0.570$   $\text{GeV}^{-1}$  and  $0.460$   $\text{GeV}^{-1}$  for the three different  $\tau$  lepton masses  $m_\tau = 1.5$  GeV, 2.0 GeV and 2.5 GeV, respectively. We then search for the roots of the vanishing derivative

$$D(m_Q) = \frac{d}{d\omega} \frac{J_0\left(2\omega\sqrt{m_Q^2 - m_\tau^2}\right)}{J_0\left(2\omega\sqrt{m_F^2 - m_\tau^2}\right)} \Big|_{\omega=\bar{\omega}} = 0, \quad (56)$$

where the  $\omega$ -independent factors in Eq. (53) have been dropped. The dependencies of the above derivative on  $m_Q$  for the three values of  $\bar{\omega}$  are exhibited in Fig. 10, where the first roots located at  $m_Q = m_F$  have no physical significance, and the second roots read  $m_Q = 3.0$  GeV, 4.0 GeV and 4.9 GeV for  $\bar{\omega} = 0.748$   $\text{GeV}^{-1}$ ,  $0.570$   $\text{GeV}^{-1}$  and  $0.460$   $\text{GeV}^{-1}$  ( $m_\tau = 1.5$  GeV, 2.0 GeV and 2.5 GeV), respectively. It is observed that the  $\tau$  lepton must have a mass around 2 GeV in order to produce the bottom quark mass  $m_b = 4.03$  GeV, the same as that extracted from the  $Q \rightarrow c\bar{u}\bar{d}$  decay width. To be precise, the  $\tau$  lepton takes the mass  $m_\tau = 2.02$  GeV. A lower (higher)  $m_\tau$  would lead to a lower (higher)  $m_b$ . The value  $m_\tau = 2.02$  GeV, deviating from the measured one  $m_\tau = 1.777$  GeV [55] by 14%, is satisfactory enough in the current preliminary attempt. Following the prescription for estimating the uncertainty involved in the  $Q \rightarrow s\bar{u}\bar{d}$  decay, we determine the  $\tau$  lepton mass  $m_\tau = (2.02 \pm 0.02)$  GeV, where the error comes from the allowed range of  $\bar{\omega}$ . We remark that the above analysis is independent of the effective gluon mass  $m_g$  in the absence of the Wilson coefficients, so the constraint on  $m_\tau$  is quite rigid. Similarly, we emphasize the nontrivial and stringent correlation among the concerned masses, instead of their exact values.

The dependencies of the subtracted width  $\Delta\Gamma_s(m_Q)$  and the width  $\Gamma_s(m_Q)$  on  $m_Q$  are displayed for three values of  $\omega$  around  $\bar{\omega} = 0.570$   $\text{GeV}^{-1}$ , i.e.,  $\omega = 0.52$   $\text{GeV}^{-1}$ ,  $0.570$   $\text{GeV}^{-1}$  and  $0.62$   $\text{GeV}^{-1}$ , in Figs. 11(a) and 11(b), respectively. The CKM factor  $|V_{\text{CKM}}|^2 = |V_{ub}|^2$  has been included with  $|V_{ub}| = A\lambda^3\sqrt{\bar{\rho}^2 + \bar{\eta}^2}$ , where the Wolfenstein parameters



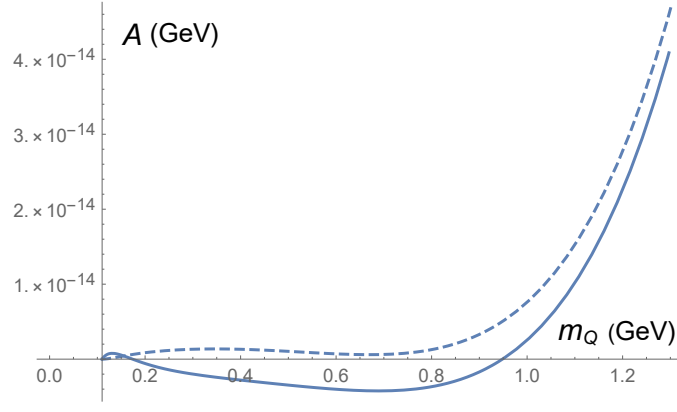


FIG. 12: The HQE widths of the semileptonic decay  $Q \rightarrow d\mu^+\nu_\mu$  divided by the CKM factor,  $A(m_Q) \equiv \Gamma_s^{\text{HQE}}(m_Q)/|V_{\text{CKM}}|^2$ , with (solid line) and without (dashed line) the dimension-seven contribution.

take the values  $\bar{\rho} = 0.159$  and  $\bar{\eta} = 0.348$  [55]. The diminishing of  $\Gamma_s(m_Q)$  for  $m_Q > m_\tau$  up to  $m_Q \approx 2.5$  GeV in Fig. 11(b) certifies the superb coincidence between  $\Delta\Gamma_s(m_Q)$  and  $-\Gamma_s^{\text{HQE}}(m_Q)$  in the interval  $(m_\tau, m_F)$ . All three curves cross each other in the small region located at  $m_Q \approx 4$  GeV in Fig. 11(a), suggesting the stability of the widths at this  $m_Q$  under the variation of  $\omega$ . Though the magnitude of  $\Delta\Gamma_s(m_Q)$  is smaller than  $\Gamma_s(m_Q)$ , the intersection of the curves is still visible in Fig. 11(b). We read off the decay widths at  $m_b \approx 4.0$  GeV:  $\Delta\Gamma_s(m_b) = 1.65 \times 10^{-17}$  GeV and  $\Gamma_s(m_b) = 8.06 \times 10^{-17}$  GeV, which also imply a minor nonperturbative contribution to  $B$  meson decays. The above prediction for  $\Gamma_s(m_b)$  is equivalent to the branching fraction  $B(b \rightarrow u\tau^-\bar{n}u\tau) = 2.0 \times 10^{-4}$ , for which no data are available so far. However, it ought to be lower than the measured  $b \rightarrow ue^-\bar{\nu}_e$  branching fraction  $1.65 \times 10^{-3}$  [55], so at least its order of magnitude makes sense.

Next we constrain the muon mass  $m_\mu$  from the dispersion relation for the semileptonic decay  $Q \rightarrow d\mu^+\nu_\mu$ . As stated before, the destructive dimension-seven contribution renders the HQE width slightly negative in the low  $m_Q$  region. To be quantitative, we display the HQE width divided by the CKM factor,  $A(m_Q) \equiv \Gamma_s^{\text{HQE}}(m_Q)/|V_{\text{CKM}}|^2$ , with and without the dimension-seven contribution in Fig. 12, where the muon mass has been set to  $m_\mu = 0.1$  GeV for illustration. The binding energy is kept as  $\bar{\Lambda} = 0.5$  GeV. It is seen that the former is negative in the range  $0.15 \text{ GeV} < m_Q < 0.95 \text{ GeV}$ . Because the dimension-seven contribution is not yet complete, it is likely that this unphysical result would be amended in a full calculation. One possibility to go around this annoyance is to neglect the dimension-seven contribution, which is the least leading one in the HQE anyway. With the HQE input up to the dimension-six weak annihilation contribution, Eq. (8) becomes, in the limit  $m_Q \rightarrow m_\ell$ ,

$$\Gamma_s^{(6)+(7)}(m_Q) \propto \frac{3(m_Q^2 - m_\ell^2)^2 m_\ell^2}{m_Q^3} \left(1 + \frac{\bar{\Lambda}}{m_Q}\right), \quad (57)$$

where the second term in the parentheses comes from the expansion  $m_{H_Q} = m_Q + \bar{\Lambda}$  for the dimension-six piece. The similar procedure yields the solution

$$\Delta\Gamma_s(m_Q) \approx y_e \left(1 + \frac{y_o}{y_e} m_Q\right) \frac{(m_Q^2 - m_\mu^2)^2}{m_Q^4} \left(\omega \sqrt{m_Q^2 - m_\mu^2}\right)^\alpha J_\alpha \left(2\omega \sqrt{m_Q^2 - m_\mu^2}\right), \quad (58)$$

which is fixed to  $-\Gamma_s^{\text{HQE}}(m_Q)$  in the interval  $(m_\mu, m_F)$  of  $m_Q$  with  $m_F = m_{\pi^0} + m_\mu$ .

Comparing Eqs. (57) and (58) in the limit  $m_Q \rightarrow m_\mu$ , we set the index  $\alpha = 0$  and the ratio

$$\frac{y_o}{y_e} = \frac{1}{\bar{\Lambda}} = 2.0 \text{ GeV}^{-1}. \quad (59)$$

The boundary condition at  $m_Q = m_F$  specifies the overall coefficient

$$y_e = -\Gamma_s^{\text{HQE}}(m_F) \left[ \left(1 + \frac{m_F}{\bar{\Lambda}}\right) \frac{(m_F^2 - m_\mu^2)^2}{m_F^4} J_0 \left(2\omega \sqrt{m_F^2 - m_\mu^2}\right) \right]^{-1}. \quad (60)$$

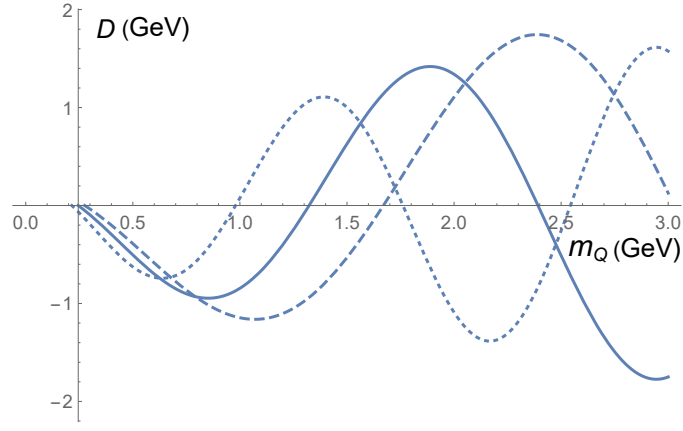


FIG. 13: Dependencies of  $D(m_Q)$  in Eq. (56) on  $m_Q$  for the  $Q \rightarrow d\mu^+\nu_\mu$  decay with  $m_\mu = 0.08$  GeV (dotted line),  $0.11$  GeV (solid line) and  $0.14$  GeV (dashed line).

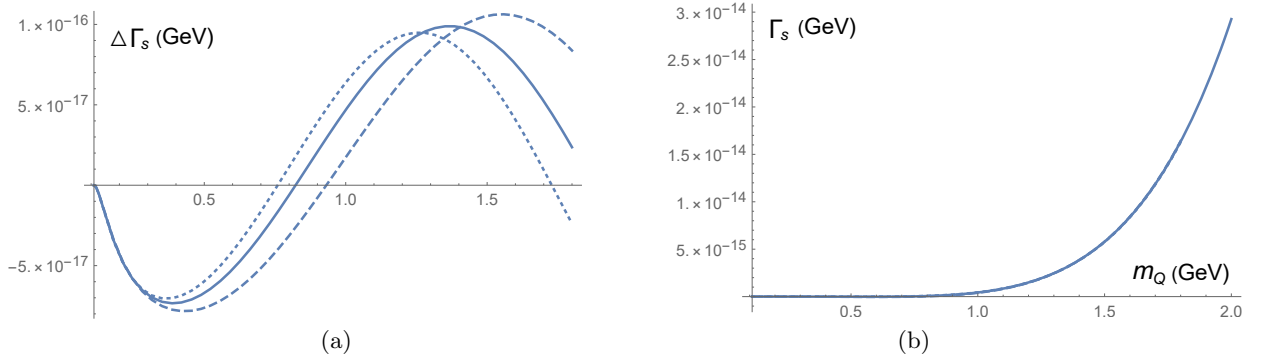


FIG. 14: Dependencies of (a) the subtracted width  $\Delta\Gamma_s(m_Q)$  and (b) the width  $\Gamma_s(m_Q)$  of the  $Q \rightarrow d\mu^+\nu_\mu$  decay on  $m_Q$  for  $\omega = 1.3$   $\text{GeV}^{-1}$  (dashed line),  $1.475$   $\text{GeV}^{-1}$  (solid line) and  $1.6$   $\text{GeV}^{-1}$  (dotted line).

Matching Eq. (58) to  $-\Gamma_s^{\text{HQE}}(m_Q)$  in the interval  $(m_\mu, m_F)$  determines the parameter  $\bar{\omega} = 2.008$   $\text{GeV}^{-1}$ ,  $1.475$   $\text{GeV}^{-1}$  and  $1.163$   $\text{GeV}^{-1}$  for the three different muon masses  $m_\mu = 0.08$  GeV,  $0.11$  GeV and  $0.14$  GeV, respectively. The fit does not involve the effective gluon mass  $m_g$  in the absence of the Wilson coefficients.

The stability of the solved decay width requests the vanishing derivative in Eq. (56) with  $m_\tau$  being replaced by  $m_\mu$ . The dependence of the derivative on  $m_Q$  is plotted in Fig. 13, where the second roots  $m_c = 0.98$  GeV,  $1.32$  GeV and  $1.67$  GeV corresponding to  $m_\mu = 0.08$  GeV,  $0.11$  GeV and  $0.14$  GeV, respectively, endow the decay width with the maximal stability under the variation of  $\omega$ . A lower (higher) lepton mass  $m_\mu$  would lead to a lower (higher)  $m_c$ . It is obvious that the muon mass  $m_\mu = 0.11$  GeV is preferred, because the resultant  $m_c = 1.32$  GeV is very close to  $1.35$  GeV extracted from the hadronic decay widths. We would like to make explicit that the choice  $m_\mu = 0.112$  GeV reproduces  $m_c = 1.35$  GeV exactly. It is amazing that the determined muon mass deviates from the measured value  $0.106$  GeV [55] by only about 6%. It is also noticed that the locations of the roots are very sensitive to the values of  $m_\mu$ , supporting the effectiveness of the dispersive constraint on the lepton masses. Following the similar prescription for estimating the uncertainty involved in the  $Q \rightarrow s\bar{u}d$  decay, we determine the muon mass  $m_\mu = (0.112 \pm 0.003)$  GeV, where the error comes from the allowed range of  $\bar{\omega}$ .

The dependencies of the subtracted width  $\Delta\Gamma_s(m_Q)$  in Eq. (58) and the width  $\Gamma_s(m_Q)$  on  $m_Q$  are exhibited in Figs. 14(a) and 14(b), respectively, for three values of  $\omega$  around  $\bar{\omega}$  from the best fit:  $\omega = 1.3$   $\text{GeV}^{-1}$ ,  $1.475$   $\text{GeV}^{-1}$  and  $1.6$   $\text{GeV}^{-1}$ . The CKM factor  $|V_{\text{CKM}}|^2 = |V_{cd}|^2$  has been included. The curves have a shape similar to that of the  $Q \rightarrow u\tau^+\bar{\nu}_\tau$  decay. The diminishing  $\Gamma_s(m_Q)$  for  $m_Q > m_\mu$  up to  $m_Q \approx 0.9$  GeV in Fig. 14(b) evinces the perfect match between  $\Delta\Gamma_s(m_Q)$  and  $-\Gamma_s^{\text{HQE}}(m_Q)$  in the interval  $(m_\mu, m_F)$ . The three curves cross each other more tightly at  $m_Q \approx 1.3-1.4$  GeV in Fig. 14(a), implying the stability of the widths evaluated around this  $m_Q$  under the variation of  $\omega$ . Since the magnitude of  $\Delta\Gamma_s(m_Q)$  is much lower than  $\Gamma_s(m_Q)$ , the three curves overlap almost exactly in Fig. 14(b). We read off the decay widths at  $m_c \approx 1.35$  GeV:  $\Delta\Gamma_s(m_c) \approx 1 \times 10^{-16}$  GeV and  $\Gamma_s(m_c) \approx 3 \times 10^{-15}$  GeV. The negligible  $\Delta\Gamma_s(m_Q)$  hints a tiny nonperturbative contribution to  $D$  meson semileptonic decays, distinct

from the case of hadronic decays. The predicted  $\Gamma_s(m_c)$  amounts to the branching fraction  $B(c \rightarrow d\mu^+\nu_\mu) \approx 5 \times 10^{-3}$ . The sum of the branching fractions  $3.50 \times 10^{-3}$ ,  $1.04 \times 10^{-3}$ ,  $2.4 \times 10^{-3}$  and  $1.77 \times 10^{-3}$  for the  $(\pi^0, \eta, \rho^0, \omega)\mu^+\nu_\mu$  modes, respectively, gives  $8.71 \times 10^{-3}$ , not far from our prediction.

#### IV. CONCLUSION

We have shown that dispersive analyses of physical observables can disclose stringent connections on high-energy and low-energy dynamics in the SM. It has been elaborated that the dispersion relations for inclusive heavy quark decay widths, whose definitions involve flavor-changing four-quark operators, correlate initial heavy quark masses and light final-state masses originating from the chiral symmetry breaking. The dispersion relation was reformulated in terms of the subtracted decay width, i.e., the difference between the unknown width and the HQE width. A solution to the subtracted decay width was then constructed as an expansion of the generalized Laguerre polynomials, which satisfies the initial condition from the HQE input in the interval bounded by the quark- and hadron-level thresholds. Two arbitrary parameters were introduced into the formalism: the lowest degree  $N$  for the polynomial expansion and the variable  $\Lambda$ , which scales the heavy quark mass in dispersive integrals. A solution to the dispersion relation should be insensitive to  $\Lambda$ , and this is possible only when a heavy quark takes a specific mass. A crucial feature is that the solution depends on the ratio  $\omega^2 = N/\Lambda$ . Once the solution with a physical heavy quark mass is established, both  $N$  and  $\Lambda$  can be extended to arbitrarily large values by keeping  $\omega$  in the stability window. All the large  $N$  approximations assumed in solving the dispersion relation are then justified.

Starting with massless up and down quarks, we have determined the charm and bottom quark masses from the dispersion relations for the hadronic decays  $Q \rightarrow du\bar{d}$  and  $Q \rightarrow c\bar{u}d$ , respectively. The strange quark, muon and  $\tau$  lepton masses were constrained by the dispersion relations for the  $Q \rightarrow su\bar{d}$ ,  $Q \rightarrow d\mu^+\nu_\mu$  and  $Q \rightarrow u\tau^-\bar{\nu}_\tau$  decay widths, respectively, to generate the same parent heavy quark masses. It is clear that the chiral symmetry breaking plays an important role here, without which the initial interval bounded by the quark- and hadron-level thresholds shrinks, the solution for a subtracted decay width becomes identically zero, and no constraint can be imposed on the considered fermion masses. It has been scrutinized that the decay widths corresponding to the physical heavy quark masses agree with the available data. Except that the  $Q \rightarrow du\bar{d}$  decay width is sensitive to the effective gluon mass, which is employed to stabilize the Wilson evolution to a low scale, the other channels are insensitive to the involved parameters. The observations made in this work are thus quite robust. We emphasize that no a priori information of a specific heavy quark was included: the fictitious mass  $m_Q$  in the HQE expressions for the decay widths is arbitrary. All the inputs, such as the binding energy of a heavy meson, the HQET parameters and the effective gluon mass, take typical values. Therefore, the emergence of the charm and bottom quark masses in the stable solutions, their correlations with the strange quark, muon and  $\tau$  lepton masses, and the consistency of the predicted decay widths with the data, are highly nontrivial.

Our goal is not to achieve an exact fit to the measured quantities, but to demonstrate that at least the fermion masses around the GeV scale, which characterize strong and weak dynamics, can be understood by means of the internal consistency of the SM, and that the dispersion relations for heavy quark decay widths strongly constrain those masses. No new symmetries or models beyond the SM, as attempted intensively in the literature, are needed. A more precise investigation can be invoked straightforwardly by taking into account subleading contributions to the HQE inputs, including those to the effective weak Hamiltonian, and more accurate HQET parameters and bag parameters. Though the present work is restricted to the fermion masses, the outcome has been convincing enough for conjecturing that other SM parameters can be also explained via the internal dynamical consistency, which wait for further exploration.

#### Acknowledgments

We thank H.Y. Cheng for helpful discussions. This work was supported in part by National Science and Technology Council of the Republic of China under Grant No. MOST-110-2112-M-001-026-MY3.

- 
- [1] C. D. Froggatt and H. B. Nielsen, Nucl. Phys. **B147**, 277–298 (1979).
  - [2] F. Feruglio, arXiv:1706.08749 [hep-ph].
  - [3] X. K. Du and F. Wang, JHEP **01**, 036 (2023).
  - [4] S. T. Petcov and M. Tanimoto, arXiv:2212.13336 [hep-ph].

- [5] S. Kikuchi, T. Kobayashi, K. Nasu, S. Takada and H. Uchida, Phys. Rev. D **107**, no.5, 055014 (2023).
- [6] I. Bree, S. Carrolo, J. C. Romao and J. P. Silva, Eur. Phys. J. C **83**, no.4, 292 (2023).
- [7] Y. Abe, T. Higaki, J. Kawamura and T. Kobayashi, arXiv:2301.07439 [hep-ph].
- [8] N. Seiberg, Phys. Rev. D **49**, 6857-6863 (1994).
- [9] N. Seiberg, Nucl. Phys. B **435**, 129-146 (1995).
- [10] S. S. Razamat and D. Tong, Phys. Rev. X **11**, 011063 (2021).
- [11] Y. Hamada and J. Wang, [arXiv:2209.15244 [hep-ph]].
- [12] N. Arkani-Hamed and M. Schmaltz, Phys. Rev. D **61**, 033005 (2000).
- [13] G. F. Giudice and M. McCullough, JHEP **02**, 036 (2017).
- [14] N. Craig, I. Garcia Garcia and D. Sutherland, JHEP **10**, 018 (2017).
- [15] H. n. Li, Phys. Rev. D **107**, no.5, 054023 (2023).
- [16] M. A. Shifman, A. I. Vainshtein and V. I. Zakharov, Nucl. Phys. B **147**, 385 (1979); B **147**, 448 (1979).
- [17] H. n. Li, H. Umeeda, F. Xu and F. S. Yu, Phys. Lett. B **810**, 135802 (2020).
- [18] A. S. Xiong, T. Wei and F. S. Yu, arXiv:2211.13753 [hep-th].
- [19] H. n. Li, Phys. Rev. D **104**, 114017 (2021).
- [20] J. Gratrex, B. Melić and I. Nišandžić, JHEP **07**, 058 (2022).
- [21] T. Blum, A. Soni and M. Wingate, Phys. Rev. D **60**, 114507 (1999).
- [22] C. A. Dominguez, N. F. Nasrallah, R. Rontsch and K. Schilcher, JHEP **05**, 020 (2008).
- [23] Y. Amhis *et al.* [HFLAV], Phys. Rev. D **107**, no.5, 052008 (2023).
- [24] H. Y. Cheng, JHEP **11**, 014 (2018).
- [25] H. n. Li and H. Umeeda, Phys. Rev. D **102**, no.9, 094003 (2020).
- [26] H. n. Li and H. Umeeda, Phys. Rev. D **102**, 114014 (2020).
- [27] H. n. Li, Phys. Rev. D **106**, no.3, 034015 (2022).
- [28] A. Lenz and T. Rauh, Phys. Rev. D **88**, 034004 (2013).
- [29] V. A. Khoze, M. A. Shifman, N. G. Uraltsev and M. B. Voloshin, Sov. J. Nucl. Phys. **46**, 112 (1987) [Yad. Fiz. **46**, 181 (1987)].
- [30] J. Chay, H. Georgi and B. Grinstein, Phys. Lett. B **247**, 399 (1990).
- [31] A. Lenz, M. L. Piscopo and A. V. Rusov, [arXiv:2208.02643 [hep-ph]].
- [32] F. Bernlochner, M. Fael, K. Olschewsky, E. Persson, R. van Tonder, K. K. Vos and M. Welsch, JHEP **10**, 068 (2022).
- [33] I. I. Y. Bigi, N. G. Uraltsev and A. I. Vainshtein, Phys. Lett. B **293**, 430-436 (1992) [erratum: Phys. Lett. B **297**, 477-477 (1992)].
- [34] A. F. Falk, Z. Ligeti, M. Neubert and Y. Nir, Phys. Lett. B **326**, 145-153 (1994).
- [35] T. Mannel, A. V. Rusov and F. Shahriaran, Nucl. Phys. B **921**, 211-224 (2017).
- [36] H. K. Quang and X. Y. Pham, Phys. Lett. B **122**, 297 (1983).
- [37] Y. Nir, Phys. Lett. B **221**, 184 (1989).
- [38] E. Bagan, P. Ball, V. M. Braun and P. Gosdzinsky, Nucl. Phys. B **432**, 3-38 (1994).
- [39] E. Bagan, P. Ball, V. M. Braun and P. Gosdzinsky, Phys. Lett. B **342**, 362-368 (1995) [erratum: Phys. Lett. B **374**, 363-364 (1996)].
- [40] E. Bagan, P. Ball, B. Fiol and P. Gosdzinsky, Phys. Lett. B **351**, 546-554 (1995).
- [41] M. Neubert and C. T. Sachrajda, Nucl. Phys. B **483**, 339-370 (1997).
- [42] N. G. Uraltsev, Phys. Lett. B **376**, 303-308 (1996).
- [43] M. Beneke and G. Buchalla, Phys. Rev. D **53**, 4991-5000 (1996).
- [44] E. Franco, V. Lubicz, F. Mescia and C. Tarantino, Nucl. Phys. B **633**, 212-236 (2002).
- [45] M. Beneke, G. Buchalla, C. Greub, A. Lenz and U. Nierste, Nucl. Phys. B **639**, 389-407 (2002).
- [46] D. King, A. Lenz, M. L. Piscopo, T. Rauh, A. V. Rusov and C. Vlahos, JHEP **08**, 241 (2022).
- [47] A. F. Falk, Y. Grossman, Z. Ligeti, Y. Nir and A. A. Petrov, Phys. Rev. D **69**, 114021 (2004).
- [48] D. Borwein, J. M. Borwein, R. E. Crandall, SIAM J. Numer. Anal. **46**, 3285-3312 (2008).
- [49] M. Kirk, A. Lenz and T. Rauh, JHEP **12**, 068 (2017) [erratum: JHEP **06**, 162 (2020)].
- [50] D. King, A. Lenz and T. Rauh, JHEP **06**, 134 (2022).
- [51] G. Buchalla, A. J. Buras and M. E. Lautenbacher, Rev. Mod. Phys. **68**, 1125-1144 (1996).
- [52] T. Zhong, Z. H. Zhu, H. B. Fu, X. G. Wu and T. Huang, Phys. Rev. D **104**, 016021 (2021).
- [53] A. C. Aguilar, D. Binosi and J. Papavassiliou, Front. Phys. (Beijing) **11**, no.2, 111203 (2016).
- [54] J. D. Gomez and A. A. Natale, Int. J. Mod. Phys. A **32**, no.02n03, 1750012 (2017).
- [55] R.L. Workman et al. (Particle Data Group), Prog. Theor. Exp. Phys. 2022, 083C01 (2022).